ONTARIO GEOLOGICAL SURVEY

Open File Report 5560

The Mechanical Properties of the Kettle Point Oil Shales

by

M. B. Dusseault and M. Loftsson

1985

THIS PROJECT WAS PART OF THE HYDROCARBON ENERGY RESOURCES PROGRAM (HERP), AND WAS FUNDED BY THE ONTARIO MINISTRY OF TREASURY AND ECONOMICS UNDER THE BOARD OF INDUSTRIAL LEADERSHIP AND DEVELOPMENT (BILD) PROGRAM.

Dusseault, M. B and Loftsson, M.

1985: The Mechanical Properties of the Kettle Point Oil Shale, Ontario Geological Survey Open File Report 5560, 93p., 36 figures, 8 tables.

Ministry of Natural Resources
Ontario

BILD
ONTARIO Ministry of Natural Resources

Ontario Geological Survey

OPEN FILE REPORT

Open File Reports are made available to the public subject to the following conditions:

This report is unedited. Discrepancies may occur for which the Ontario Geological Survey does not assume liability. Recommendations and statements of opinions expressed are those of the author or authors and are not to be construed as statements of government policy.

This Open File Report is available for viewing at the following locations:

(1) Mines Library
Ministry of Natural Resources
8th floor, 77 Grenville Street
Toronto, Ontario M5S 1B3

(2) The office of the Regional or Resident Geologist in whose district the area covered by this report is located.

Copies of this report may be obtained at the user's expense from a commercial printing house. For the address and instructions to order, contact the appropriate Regional or Resident Geologist's office(s) or the Mines Library. Microfiche copies (42x reduction) of this report are available for $2.00 each plus provincial sales tax at the Mines Library or the Public Information Centre, Ministry of Natural Resources, W-1640, 99 Wellesley Street West, Toronto.

Handwritten notes and sketches may be made from this report. Check with the Mines Library or Regional/Resident Geologist's office whether there is a copy of this report that may be borrowed. A copy of this report is available for Inter-Library Loan.

This report is available for viewing at the following Regional or Resident Geologists' offices:

Regional Geologist
458 Central Ave.
London, Ontario
N6B 2E5

V.G. Milne, Director
Ontario Geological Survey

FOREWORD

The Oil Shale Assessment Project is a component of the Hydrocarbon Energy Resources Program (HERP) which is funded by the Board of Industrial Leadership and Development (BILD). For the evaluation of the hydrocarbon resource potential of the oil shales of southern Ontario, knowledge of both the hydrocarbon content of the shales and the potential for extracting these hydrocarbons is important. This report describes results of a study of the mechanical properties of the Upper Devonian Kettle Point Formation in southwestern Ontario. This information provides a better understanding of the potential for extraction of hydrocarbons from this formation.

V.G. Milne
Director
Ontario Geological Survey

TABLE OF CONTENT

List of Figures

Figure 3.1 Classification of the Kettle Point Formation according to Deere and Miller.

List of tables

ABSTRACT

The Kettle Point Formation of southwestern Ontario was tested for mechanical behavior. The Kettle Point Formation has been correlated stratigraphically to the Antrim Formation in Michigan and the Ohio Shale south of Lake Erie. It has an important position in correlating these two much larger deposits.

The shale is a relatively strong material of low modulus ratio but with extremely weak (in tension) bedding planes. The bedding plane weakness is evidenced by general fissility of core and a tendency for vertical core to split horizontally during preparation.

The organic content is not functionally related to the strength/deformation properties in any discernable way. However, the quartz:illite ratio, as estimated from X-ray peak intensity, is strongly related to most strength/deformation properties.

We interpret this finding by observing that the kerogen contents of the Kettle Point Formation are relatively small, less than 22% by volume, and likely do not enter significantly into the rigid rock skeleton, which is dominated by the minerals quartz and illite. Given this interpretation, the relationship to quartz:illite ratios becomes logical, as greater amounts of clay minerals would be expected to reduce fabric strength, other things being equal.

Quarrying and mining of the Kettle Point Formation is entirely feasible as the material is competent and will not slake, spall, or weather rapidly in

a mine environment. The major concern is with controlling roof delamination due to bedding plane fissility. Any fluid flow in the rock will be dominated by fractures, joints, and bedding plane discontinuities, as the intact rock is of very low permeability.

ONTARIO GEOLOGICAL SURVEY

Open File Report

The Mechanical Properties of the Kettle Point Oil Shale

by

Maurice B. Dusseault[1] and Matthias Loftsson[2]

1985

This project was part of the Hydrocarbon Energy Resources Program (HERP), and was funded by the Ontario Ministry of Treasury and Economic under the Board of Industrial Leadership and Development (BILD) Program.

[1]Professor, Dept. of Earth Sciences, University of Waterloo.

[2]Graduate student, Dept. of Earth Sciences, University of Waterloo.

1.0 INTRODUCTION

1.1 General

The general study of geological materials is of fundamental importance to engineering and earth sciences. First, each material is different from others and therefore provides us with new data concerning the variability of natural strata. Secondly, each material displays a wide range of material properties, giving us insight into the heterogeneity displayed by nature. Thirdly, the integration of geological information with engineering data promotes an interdisciplinary approach which often leads to useful generalization. Study of the mechanical properties of the Kettle Point Formation has been very useful from these aspects alone.

Oil shale research has provided another, more direct, benefit. The information helps directly in the evaluation process of the oil shale as a potential multiple resource: a source of thermal energy and an aggregate resource. It is arguable whether shale oil can conceivably be competitive with conventional oil, heavy oil, or oil sands within the next decade but multiple use may lead to considerable interest in the short term. Another economically interesting aspect of oil shale development is the use of excavated space: underground storage space is increasing significantly in value for specialized liquid storage, constant temperature vault storage for surplus food stuffs, and for archiving of data in controlled environments. These multiple uses of the Kettle Point Formation make its study worthwhile.

This report does not address the potential value and use of underground space, nor does it explicitly address the use of spent shale as an aggregate or a concrete additive. Also, the explicit value of the organic matter either

as a thermal resource or as a potential source of liquid hydrocarbons cannot be explored herein. Rather, this report will address the geomechanical properties of the Kettle Point Formation. Only the intact strength and deformation properties have been explored. The occurrence and properties of natural discontinuities would have to be carefully examined before underground space evaluation could be completed. The direct comminution properties have not been determined yet; this should be done if a crushing/retorting operation is to be evaluated. Dynamic properties as related to blasting cannot easily be studied and are perhaps not too germane as any underground mining scheme is more likely to be by some continuous excavation method. Also, blastability is seldom studied directly in laboratory environments.

The mechanical strength and deformation properties we have studied can be directly related to data on other materials for which more is known. By this means, the value of the study can be extended significantly. Whether extractive operations involve underground mining, surface mining, subsurface in situ retorting, or some combination of these, knowledge and understanding of the physical and mechanical characteristics of the shale deposit is required. The laboratory testing described herein can give insight into other behavioral characteristics which will be critical in organization, planning, design, and bed preparation at the time of operation.

The estimated resources of shale oil recoverable by hydrogen retorting technology in the Michigan Basin areas is about 5 billion bbl. or about 49,000 bbl/acre. For this resource estimate four criteria for resource assessment were imposed: at least 10% organic carbon, at least 3 m thick, stripping ratio no greater than 2.5:1, and overburden less than 61 metres (Matthews, 1983). The Kettle Point Formation is geologically very closely related to the

Michigan Shales (McNamara et al., 1979), but bears a different name being on the Canadian side of the border. To our knowledge, the potential resource value of the Kettle Point Formation has not been estimated. This is a contentious exercise in any case because of the difficulty in defining what actually should be included in a potential resource evaluation. The lower cut-off grade is arguable, and the use of oil shale requires suitable technology and will be aided by multiple uses. Fisher Assay oil yield for the Kettle Point Formation is commonly between 20 - 50 litres per metric tonne, with a maximum yield of 70 l/tonne (personal communication, J.F. Barker, University of Waterloo, 1984). The oil yield by hydrogen retorting technology processes can be doubled under optimum conditions (Russell and Barker, 1983). This deposit contains much less organic matter than the United States Green River Formation, which is commonly in the 80 - 160 l/tonne range (Crookston, 1978). The resource is not of exceptional value for its oil content alone but multiple uses may hold the key for future development.

This report is divided into four sections. This first chapter is an introduction and includes this general discussion, a discussion on mineralogical and geological characteristics, and contains a brief review of prior study on the physical properties of the Antrim Formation in the United States, which is geologically and mineralogically equivalent to the Kettle Point Formation. The second chapter describes present studies, discusses the tests performed, and gives the test results. The third chapter discusses relationships and factors which could have affected the obtained results, compares the obtained and existing data along with an estimate of errors, and considers material classification. The fourth chapter summarizes the data and the last chapter recommends an approach to further study.

1.2 Geological and Mineralogical Characteristics

The Kettle Point Formation is a dark gray to black kerogenous shale. It is part of the widespread Devonian shale deposits in the eastern United States (Ohio, Michigan, Indiana, and Kentucky). The Kettle Point Formation is stratigraphically equivalent to the Antrim Formation in Michigan and the Ohio Shale south of Lake Erie, and serves a key position in correlating these two units (Russell and Barker, 1983). Areas underlain by Devonian black shales in the northeastern United States and southwestern Ontario, and gamma-ray log correlations of Kettle Point Formation, Antrim Formation, and Ohio Shale are shown on figures 1.1 and 1.2 respectively. The Kettle Point Formation in Ontario is at its maximum 70 metres thick. It underlies a large area in southwestern Ontario and outcrops only at one location, from which the formation is named, at Kettle Point on the coast of Lake Huron. Depth of overburden cover is less than 100 metres (Russell and Barker, 1983).

Mineralogical studies of the Antrim Formation have indicated that it is a fine-grained laminated shale composed mainly of quartz and the clay mineral illite. It contains minor amounts of feldspar, kaolinite, chlorite, carbonates, and pyrite (Humphrey, 1978; McNamara et al., 1979). The clay minerals occur as thin platelets less than a micron in thickness and several microns in major diameter. Quartz and feldspar occur as grains, 5 - 30 microns in size, and carbonate occurs as minute irregular grains. Pyrite ranges from large concretionary masses to very finely disseminated crystals. The organic matter occurs as finely dispersed, amorphous brown binder and as disc-shaped spore-like fossils, referred to as Tasmanites (Humphrey, 1978). Quartz and illite usually compose more than 85% by weight of the total mineral matter (Humphrey, 1978). Preliminary study on mineral composition has indicated

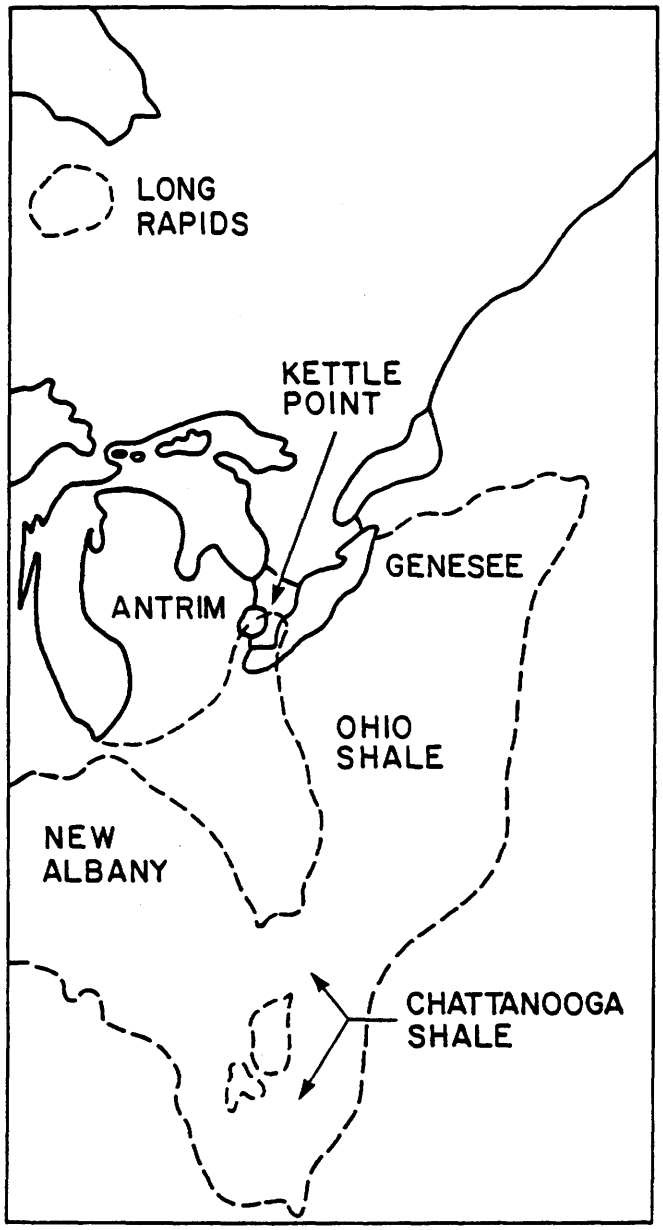

Figure 1.1 Areas underlain by black Devonian shales in northeastern United States and southwestern Ontario (Russell and Barker, 1983).

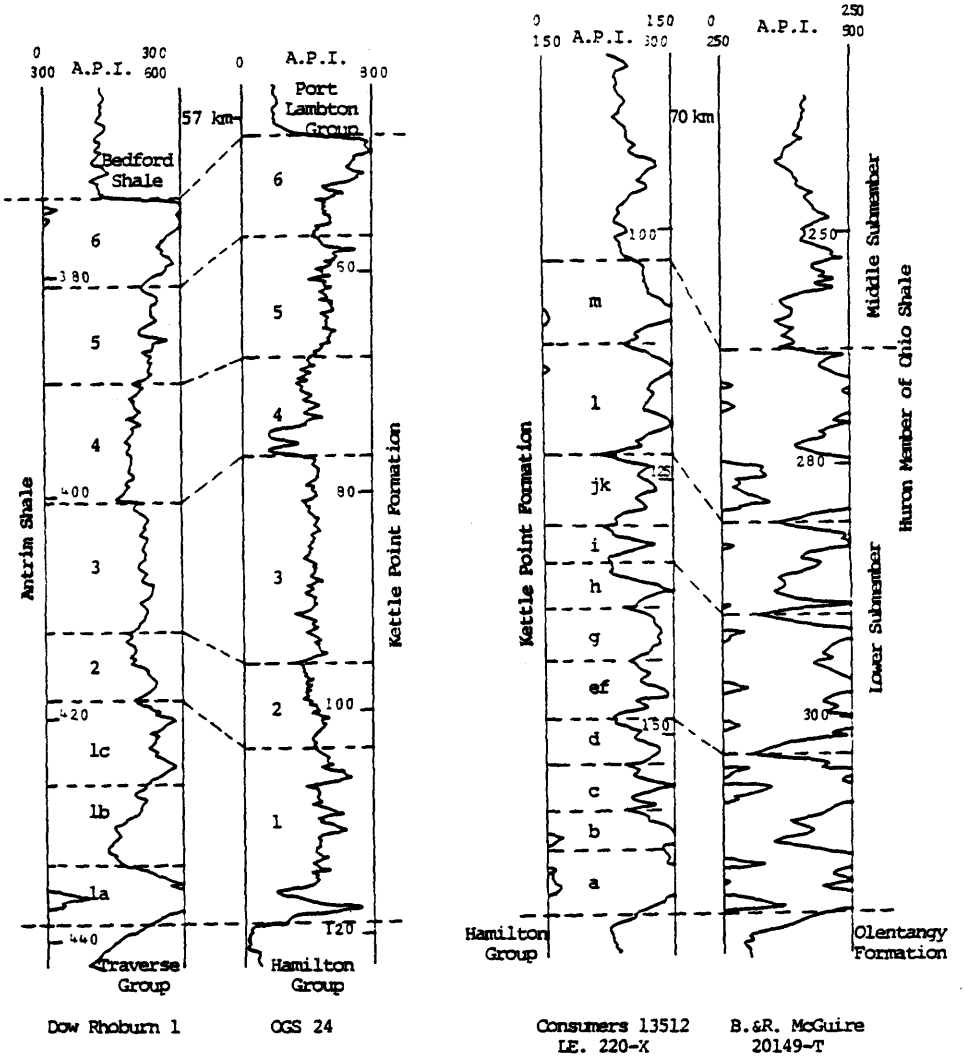

Figure 1.2 Gamma-ray log correlation of the Kettle Point Formation, Antrim Formation, and Ohio Shale (Russell and Barker, 1983).

that the above description agrees in general with the mineral composition of the Kettle Point Formation (Dusseault et al., 1983; current study by authors). The amount of organic matter (%TOC) in the Kettle Point Formation ranges from 0 - 15 percent. The nature of the organic matter is dominantly kerogen of marine origin and has only attained an immature thermal maturation stage (Barker et al., 1983).

1.3 Previous Work on Physical Characteristics

1.3.1 Green River Formation oil shale

During the past two decades, very detailed research has been performed on the Green River Formation of the western United States (Utah, Colorado, and Wyoming). Later oil shale studies have usually contrasted and compared the properties of the studied material with those of the Green River deposits. It is therefore necessary to review, briefly, the basic mechanical properties of this well-studied material. It should be noted that the Green River Formation is of terrestrial origin, a lacustrine deposit, whereas the Kettle Point Formation is of marine origin, and of grossly different mineralogy. A typical mineral composition of the Green River Formation, Mahogany Zone, is given in table 1.1.

Tests on the Green River Formation oil shale have indicated that the mechanical properties are highly influenced by the organic matter and, to a much lesser degree, mineral content (Chong et al., 1976; Chong et al., 1979a; Chong et al., Results from tensile tests and uniaxial and triaxial compression tests are commonly reported as being functionally related to the amount of organic matter, indicating decreasing strength and modulus of deformation with increasing amount of organic content (Chong et al., 1979b; Chong et al., 1982; Costin, 1981). Temperature effects, decreasing strength with increasing temperature (Closmann and Bradley, 1979; Costin, 1981), and strain rate effects, increasing strength with increasing strain rate (Chong et al., 1980), have been noted. The organic matter, however, is the rock-forming component that primarily affects the results obtained in mechanical testing, other factors being equal. The effects of varying quantities of other minerals such

	Weight-percent
Organic matter:	
Content of raw shale	13.8
Ultimate composition:	
Carbon	80.5
Hydrogen	10.3
Nitrogen	2.4
Sulfur	1.0
Oxygen	5.8
Total	100.0
Mineral matter:	
Content of raw shale	86.2
Estimated mineral constituents:	
Carbonates, principally dolomite	48.0
Feldspars	21.0
Quartz	13.0
Clays, principally illite	13.0
Analcite	4.0
Pyrite	1.0
Total	100.0

Table 1.1 A typical mineral composition of the Green River Formation, Mahogany zone (Thorne et al., 1964).

as dolomite on the strength and deformation properties of the Green River Formation are important only for specimens of low organic content.

A detailed summary of pertinent mechanical properties can be found elsewhere (Dusseault et al., 1983).

1.3.2 Antrim Formation

There is little data available on the mechanical properties of the Antrim Formation. Kim (1978) studied the mechanical characteristics of the Antrim Formation deposit in uniaxial compression, point load strength, ultrasonic velocity, and surface hardness tests. Test specimens were prepared from rock cores from three boreholes. Cap rocks, floor rocks, and oil shale were tested. Results were plotted against depth for each hole and data from some 'se-

lected' (sic) samples were correlated to percent weight loss after being roasted in air at 500^0C for about 24 hours. The weight loss was supposed to give some indication of the actual amount of organic matter. In tests we are currently performing, we have found that the oxidized zone progresses inward very slowly in Kettle Point Formation kept in an air atmosphere in a muffle furnace at 500^0C. This suggests that their methodology is in question. Unfortunately, insufficient detail is available in the published papers.

In uniaxial compression, compressive strength ranged from 56.4 - 161.0 MPa. Stress-strain curves were divided into two groups: a low modulus group, of modulus ranging from 10 - 20 GPa, and a high modulus group of 40 - 96 GPa modulus (Kim, 1978). The samples belonging to the latter group were either extremely low grade oil shale or floor rocks, but the former group consisted mainly of true oil shale samples. Poisson's Ratio ranged from 0.08 to 0.35. No samples of cap rock were tested due to the high fracture frequency in the cores. If data are plotted against percent weight loss, decreasing trends are observed for strength and modulus of deformation but scatter is very high and in fact it is doubtful if any correlation exists at all if outliers are eliminated from the data. Results are summarized graphically in figures 1.3 - 1.5.

In ultrasonic wave velocity measurements, P-wave velocity (V_p) for pure oil shale samples ranged from 2.4 - 3.5 km/sec, whereas samples with 'more than 50% intrusions of calcareous material' (sic) ranged from 5.0 - 6.0 km/sec (Kim, 1978). Dynamic values of Young's Modulus, Poisson's Ratio, and density, calculated from P- and S-wave velocities, were always higher than the static values. When the dynamic values are plotted against percent weight loss, a decreasing trend for Young's Modulus is also observed as the

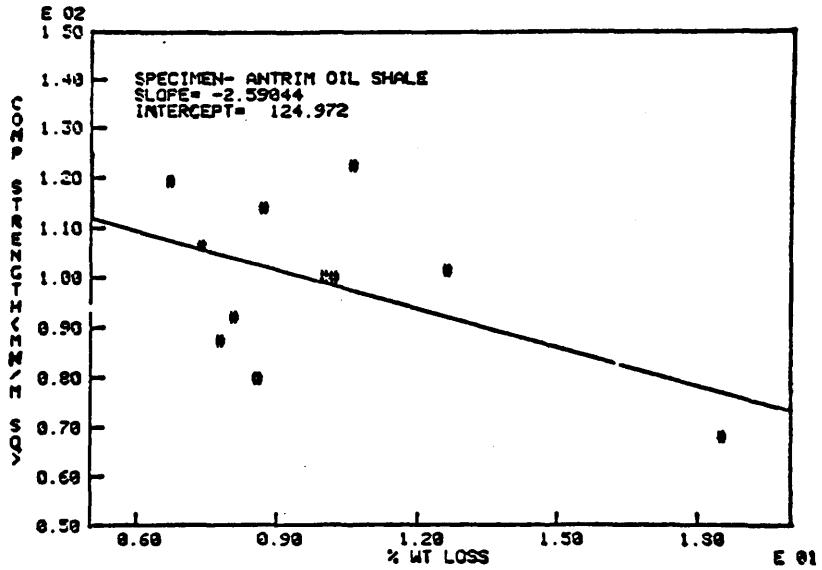

Figure 1.3 Uniaxial compressive strength versus % weight loss (Kim, 1978).

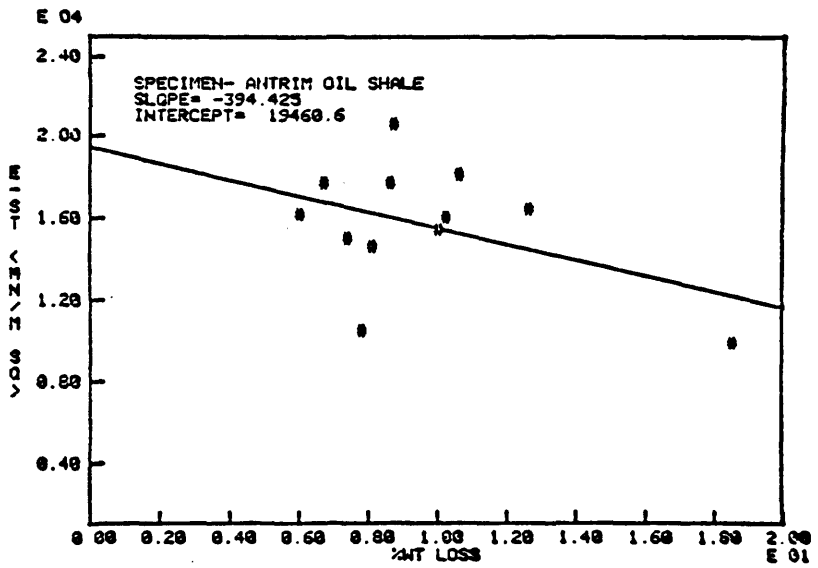

Figure 1.4 Static Young's Modulus versus % weight loss (Kim, 1978).

weight loss increases, similar to static data, but again scatter is very high. Graphical presentations of dynamic Young's Modulus and Poisson's Ratio versus % weight loss are shown on figures 1.6 and 1.7.

Point load tests gave values of the point load index ranging from 8.6 - 40.6 MPa but were most commonly in the 10 - 30 MPa range. The data provided was not plotted against percent weight loss nor is it compared with the data obtained in uniaxial compression.

In Scleroscope hardness tests, rebound hardness values ranged from 15.7 - 47.7. Data is plotted against point load strength indicating an increasing trend with increasing point load strength, a logical relationship. This relationship for one borehole is shown on figure 1.8. Statistical usefulness of the data presented on figures 1.3 - 1.8 is very limited. If outliers are eliminated from the data, coefficient of determination (r^2) becomes in many cases less than 0.1. In such cases regression lines are meaningless.

Singh et al. (1979) studied the change in mechanical properties of the Antrim Formation on retorting. The retorting procedure was simulated by roasting the samples at 500^0C in air for 48 hours. For uniaxial compression testing, duplicate samples of the same size and visual homogeneity were prepared. One was tested after the roasting procedure, the other was tested unroasted. Results are graphically presented on figure 1.9. As shown on the figure, there is a definite trend for decreasing values of strength and deformation properties upon roasting and the change becomes more pronounced with increasing percent weight loss. In this same study by Singh et al. (1979), porosity and permeability, parallel and perpendicular to the bedding planes, were measured for unroasted and roasted samples. The porosity was measured as apparent porosity, in other words, 'the ratio of the volume of

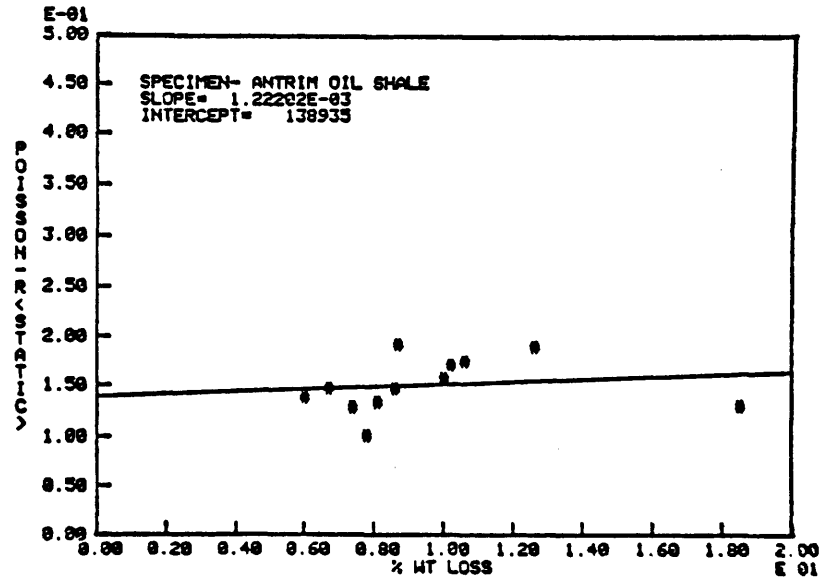

Figure 1.5 Static Poisson's Ratio versus % weight loss (Kim, 1978).

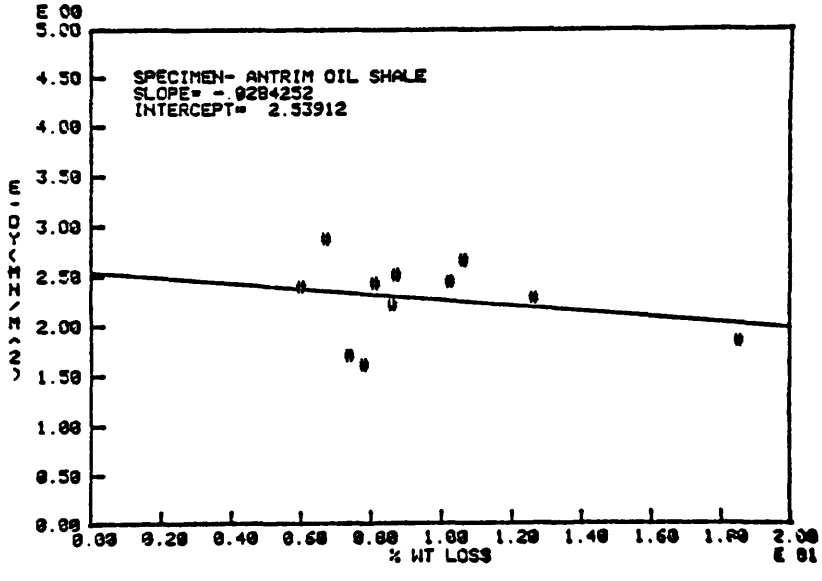

Figure 1.6 Dynamic Young's Modulus versus % weight loss (Kim, 1978).

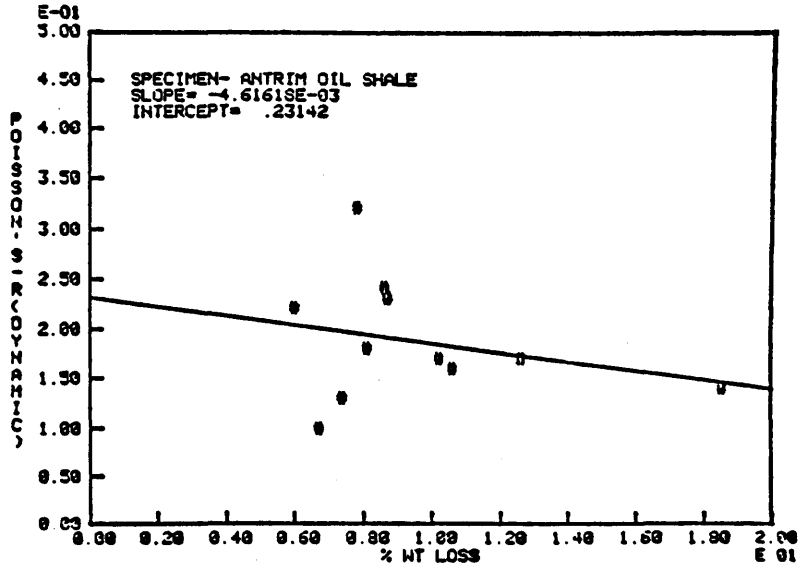

Figure 1.7 Dynamic Poisson's Ratio versus % weight loss (Kim, 1978).

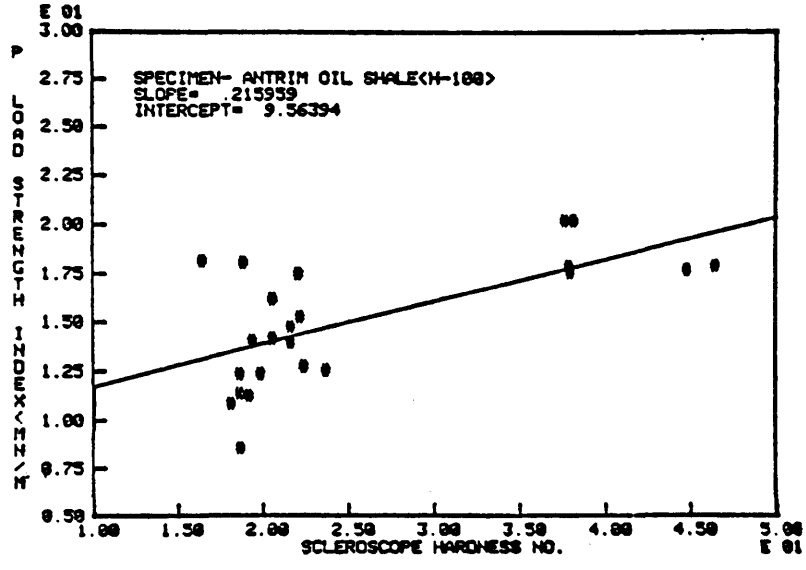

Figure 1.8 Point load strength index versus Scleroscope hardness number (Kim, 1978).

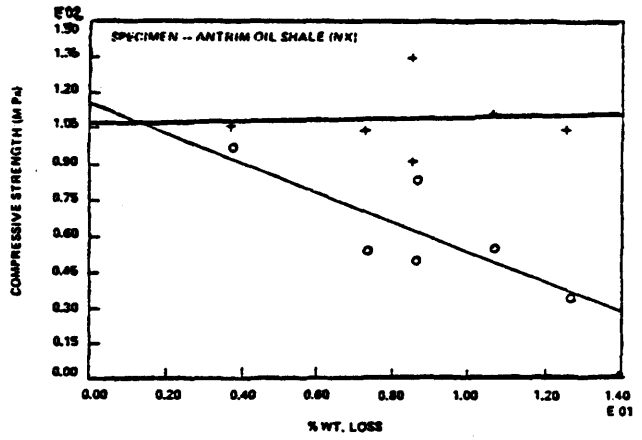

(a)

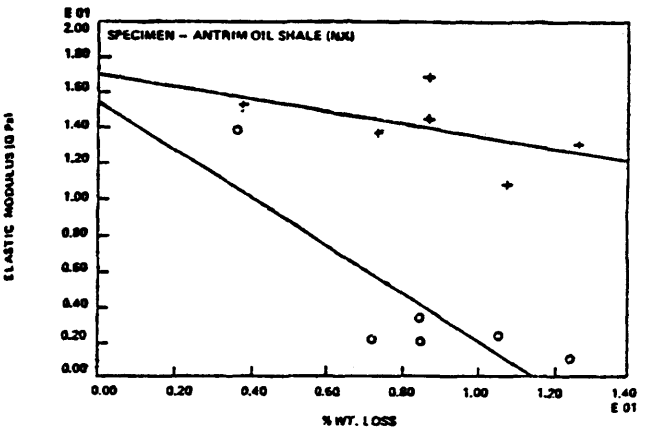

(b)

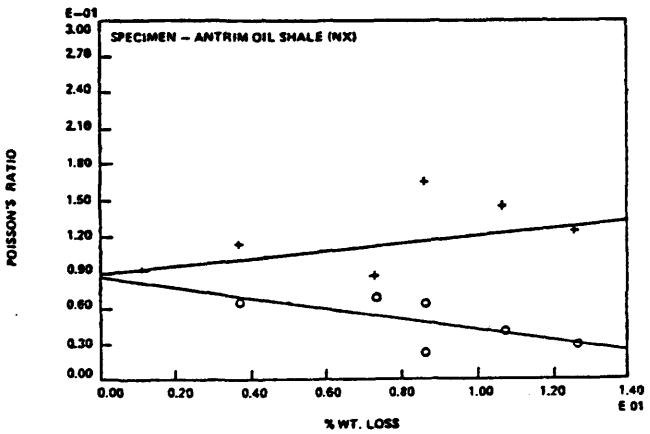

(c)

Figure 1.9 Uniaxial compressive strength (a), Young's modulus (b), and Poisson's ratio (c) of unretorted (+) and retorted (o) specimens versus percent weight loss (Singh et al., 1979).

surface-connected pores to the bulk volume'. The permeability was measured by 'recording air flow through a specimen under pressure gradient'. Results are graphically presented on figure 1.10. As shown on the figure, the change in properties again becomes more pronounced with increasing percent weight loss during roasting.

In papers by both Kim (1978) and Singh et al. (1979), percent weight loss is used as an estimate of the organic matter in the oil shale, and in a similar way to most Green River Formation studies, related to the physical and mechanical properties directly. Although discrete trends are observed, scatter is very high and in many cases any correlation that exists is solely due to outliers. In comparing these two oil shale deposits, two striking differences are noticed. The Kettle Point Formation is a very quartzitic shale with relatively low amounts of organic matter, whereas the Green River Formation is a calcareous shale moderately to very rich in organic matter.

Comparison of the organic contents of these two materials can be achieved by using statistical relationships found in the literature. First, a relationship found by Barker et al. (1983) is available:

$$FA = 4.6(TOC) - 0.73 \quad \text{(litre/tonne)} \qquad (1)$$

the parameter FA is the Fisher Assay oil yield in litres per metric ton (tonne) and TOC is the percent total organic carbon by weight. Second, a equation derived by Fordham and Dusseault (1983) has been published (see Appendix):

$$\%wt = 1.31(TOC) \qquad (2)$$

where the %wt is the percent weight loss in differential thermogravimetric analyses (DTA) between 200 and $500^{0}C$. Third, an equation was presented by Smith (1976) as:

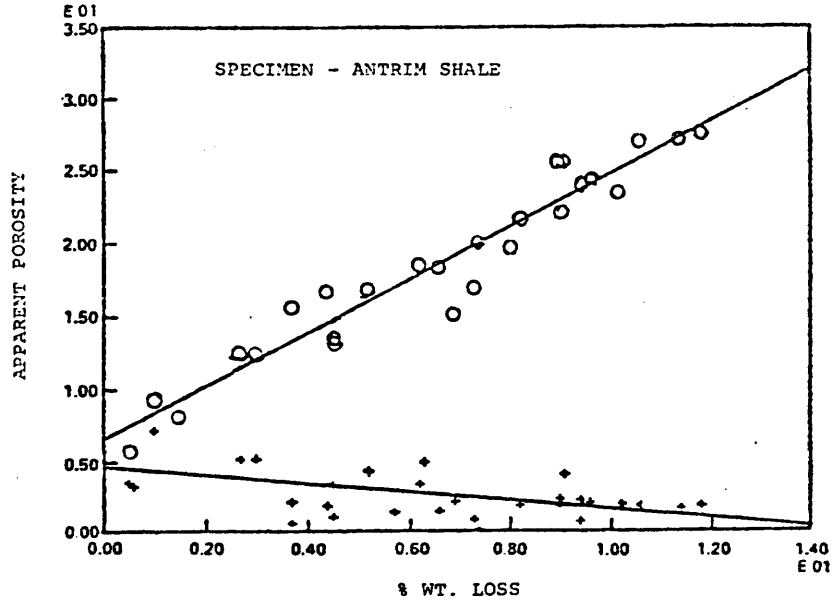

(a)

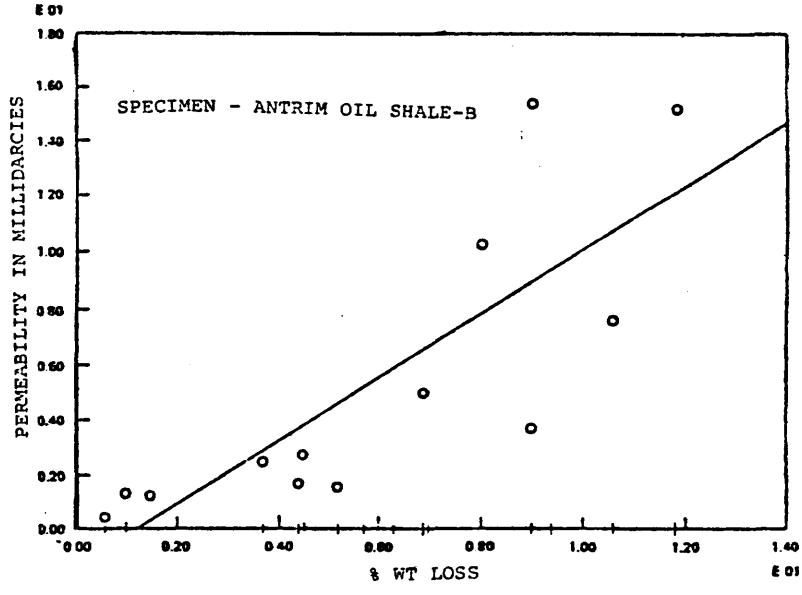

(b)

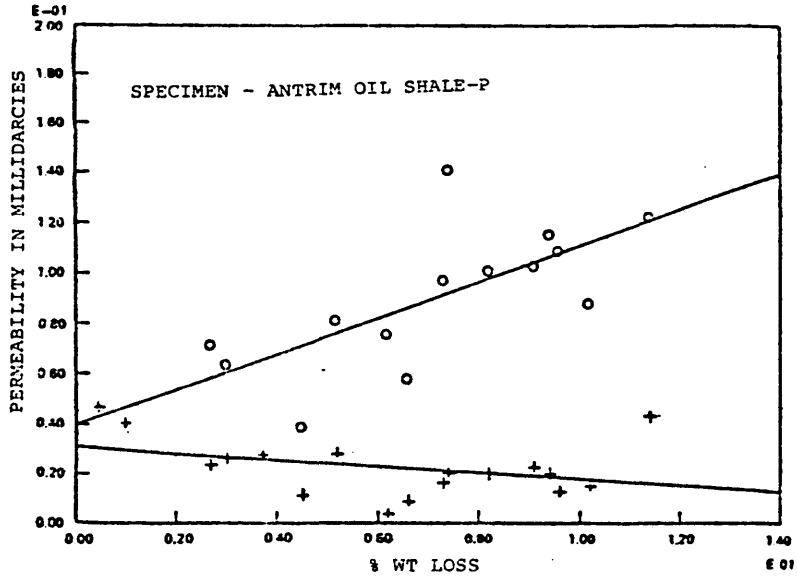

(c)

Figure 1.10 Porosity (a) and permeability parallel (b) and perpendicular (c) to bedding planes of unretorted (+) and retorted (o) specimens versus percent weight loss (Singh et al., 1979).

$$\%O_c = 157.76(M) / (0.957(M) + 107) \quad (3)$$

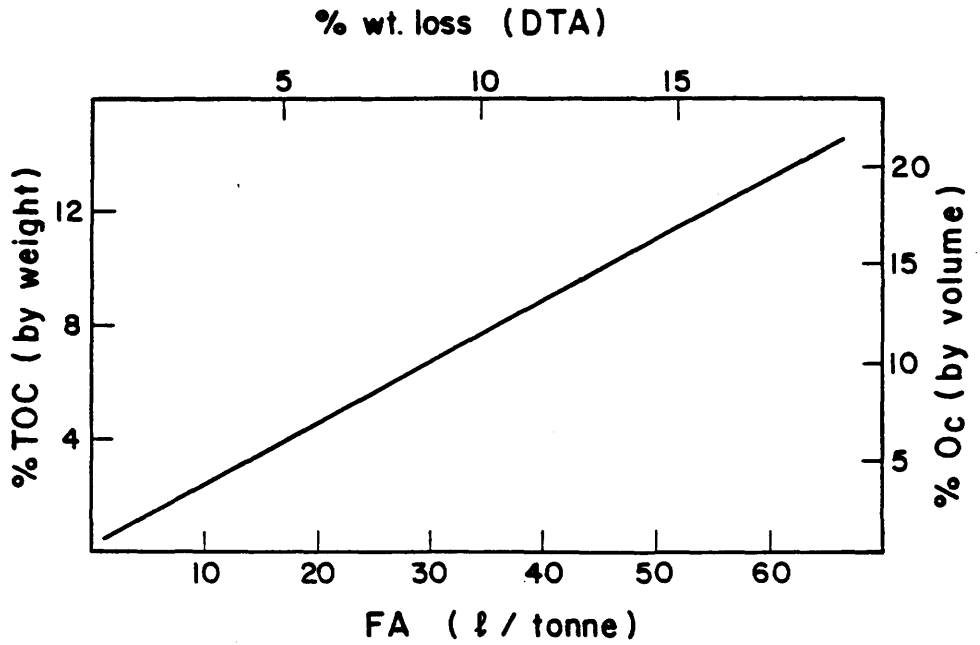

Figure 1.11 Graphical representation of the relationships given by equations 1 to 3

where M is the Fisher Assay oil yield in US-gallons per ton and %Oc is the organic volume content. The two first equations are for the Kettle Point Formation, the latter for the Green River Formation. Approximate comparisons of these equations are shown graphically on figure 1.11. By comparing data for the two materials, it is apparent that the organic content by volume (%Oc) for the Kettle Point Formation is usually less than 22% (15% TOC), whereas the %Oc for the Green River Formation is in the 10% - 60% range. Consequently, regression analyses over the small range of overlap (10% - 20% Oc) are poor, and would likely become considerably improved only if they could be extended over a wider range (10% - 60% Oc).

For the Green River Formation, the influence of dolomite and other mineral matter on strength and deformation properties is more noticeable for

oil shales containing low amounts of organic matter (< 20% Oc). For these low-grade oil shales, dolomite provides a structural support to the rock but as the %Oc increases the organic matter dilutes and weakens the dolomite matrix (Chong et al., 1976). For the Kettle Point Formation, quartz instead of dolomite provides the structural support to the rock and since this oil shale deposit always contains less than 20% Oc, the weakening effects of increasing organic matter are never felt. However, increasing amounts of clay minerals, mainly illite, in the rock matrix, damages the structural support by reducing the particle-to-particle friction and degree of interlocking of the quartz grains. Similar explanations of the quartz/clay influences on material properties can be found elsewhere (Skempton, 1964; Attewell and Taylor, 1973).

1.4 Concluding Remarks

The Kettle Point Formation is equivalent to the widespread Upper Devonian black shale deposits of the eastern United States (Antrim, Ohio, Chattanooga etc. shales Figure 1.1). The Kettle Point is a rather low grade (< 70 l/tonne) oil shale, deposited in a marine environment, and composed mainly of quartz and the clay mineral illite whereas the well-studied Green River oil shale deposit in the United States is a lacustrine, calcareous shale of much higher oil shale grade. Because of this fundamental difference, differences in the mechanical behavior can be expected and great care must be taken when studying other materials in accepting behavioral models derived for the Green River Formation.

Although prior studies of the Antrim Formation have concluded that material properties could be related to the amount of organic matter within the oil shale, no statistical proof thereof has been published. This is likely

due to a high scatter of data points and poor statistical correlation coefficients. However, a definite relationship exists between the amount of organic matter and the change in material properties upon heating. This can be explained in the following manner: quartz grains in the Antrim Formation provide a structural support to the matrix along with mica or illite platelets, but the organic matter is dispersed within the material and is found dominantly in interstices and as inactive grains. Under normal circumstances the organic matter does not influence the strength and deformation properties, but upon heating, volatilization of the organic matter (generating pressurized CO_2) and thermal expansion cause excessive cracking of the material, weakening the structural support provided by the mineral matrix. The more organic rich the oil shale, the greater the amount of fracturing and structural disruption due to the heating process. Because of similarities between the Antrim Formation and the Kettle Point Formation, the above explanation of the interaction of organic and mineral matter and material properties is very likely to be valid for the latter formation.

In the investigations described in next chapter, influences of organic matter (TOC) and minerals (X-ray diffraction intensity ratio of quartz and illite) are analyzed. Because of the poor reliability of %wt loss or %TOC as an indirect measure of material properties, a direct comparison of results obtained to those previously published is difficult. Nevertheless, certain similarities are evident, as will be pointed out in chapter 3.

2.0 MECHANICAL PROPERTIES - TEST RESULTS

2.1 General

The objective of this investigation was to determine the basic mechanical properties of the Kettle Point Formation. Tests performed were uniaxial and triaxial compression, Brazilian tension, point load index, and direct shear tests. Samples were originally collected intact at drill sites but due to the inherent weakness of the bedding planes many samples were broken during preparation. To make up for the lost samples, samples were also used which had been stored in coreboxes for up to a year. To prevent any excess water losses, all samples were wrapped in plastic and stored under humid conditions until time of testing.

Due to the extremely low porosity and permeability of this shale, measured water content of samples picked up at drill sites and samples which were stored unprotected did not vary significantly. Measured values ranged from 0.7% - 2.2% (corresponds to porosity of 1.8% - 5.5% for Gs = 2.65 and full saturation) which is within the porosity range determined by Singh et al. (1979) where porosity, in the 3% - 12% weight loss range, is 0.2% - 5.2%. Based on these results, the degree of saturation can be roughly estimated as being 50% - 90%. The actual saturation in the ground at depth can be assumed to be 100%, as there is no reasonable mechanism to explain why these shales should be unsaturated well below the groundwater table unless free methane is present. In fact, the presence of methane gas was experienced by drillers during the coring of boreholes, especially at the top of the Kettle Point Formation (personal communication, D. Russell, 1984, Ontario Geological Survey). Reduced saturation arises because of some volume

expansion on sampling, and because of loss of moisture during the drilling procedure and during the preparation of the samples for the tests when the samples are exposed to the relatively dry laboratory environment.

For each sample tested, water content and total organic carbon content (TOC) were measured and X-ray mineralogical analyses performed. The TOC analyses were carried out by combustion of powdered samples in an oxygen stream at $900^{o}C$ and by performing infrared analyses of the vaporized carbon dioxide (CO_2). Prior to the combustion process, samples are digested in hydrochloric acid (HCl) to get rid of most of the inorganic carbon which is in the form of carbonate minerals. This carbon escapes by evolution of CO_2 Series of tests have indicated that error involved is no more than 5% of the actual TOC-value.

The X-ray diffraction analyses were made to investigate mineral effects on mechanical properties and to relate to material properties obtained by different tests. The X-ray diffraction analyses were carried out by spreading a dispersion of finely powdered oil shale sample and deionized water on a ceramic tile sited on a suction bottle. After being dried at room temperature for 24 hours, the tile with the sample on top was placed in the X-ray chamber for diffraction analyses. This method gives a much better and more distinct diffraction pattern for clay minerals than the conventional powder method. Tests indicated that diffraction patterns originating from the ceramic tile did not interfere with the obtained intensities. The sample material covered the tile sufficiently to bury these patterns in the background values.

It is concluded that the organic content analysis and the X-ray diffraction give consistent, reliable, and repeatable data useable in correlation stud-

ies to other test data.

2.2 Brazilian Tensile Test Data

2.2.1 Sample preparation and test procedure

For sample preparation, ISRM suggested methods were used as a guideline (Bieniawski and Hawkes, 1977). Samples were cut from the provided rock cores at a ratio of thickness to diameter of approximately one half. Ends were ground to make them flat and parallel to within 0.25 degrees; i. e., allowing variations in thickness of less than 0.2 mm. Dimensions of the samples were determined to the nearest 0.1 mm and recorded along with a brief sample description. Samples were loaded at a displacement rate of 0.004 cm/sec (0.1 in/min) or approximately 9×10^{-4} sec^{-1} and load versus displacement monitored on a X-Y chart recorder. The compressive load was applied parallel to bedding and only samples that displayed vertical splitting were taken as representative data. This is in accordance with the use of the Brazilian disc test as an indirect measure of tensile strength. Failures other than vertical splitting are mixed-mode and cannot be interpreted directly. No strain gauges were attached to the samples, hence no information was obtained on the tensile elastic parameters, although this type of deformation data is considered contentious in any case.

2.2.2. Test results

Test results are presented in table 2.1. Tensile strength (σ_t) is calculated using the equation presented by Hondros (1959):

$$\sigma_t = -F/(\pi r t) \qquad (4)$$

where F is the compressive load at failure, r is the initial radius of the disc

SAMPLE NO	BOREHOLE	DEPTH (M)	σ_t (MPa)	%TOC	I_Q/I_I
B-1	KP-22	15.00.15.02	8.8	7.1	6.6
B-2	KP-27	11.19-11.21	10.9	8.5	11.1
B-3	KP-22	13.74-13.76	9.3	6.0	8.3
B-4	KP-28	16.30-16.32	11.5	7.1	8.0
B-5	KP-28	21.98-22.00	10.2	5.7	10.8
B-6	KP-27	22.13-22.15	9.2	9.0	9.4
B-7	KP-22	24.33-24.35	16.5	4.0	16.6
B-8	KP-22	14.85-14.87	8.2	6.3	7.8
B-9	KP-22	14.94-14.96	10.1	7.6	8.9
B-10	KP-22	14.98-15.00	9.5	7.5	8.6
B-11	KP-23	21.55-21.57	7.2	7.0	9.6
B-12	KP-23	37.94-37.96	10.8	9.2	10.3
B-13	KP-27	29.93-29.95	10.0	5.8	9.1
B-14	KP-27	29.95-29.97	11.9	4.8	8.9
B-15	KP-23	26.49-26.51	8.4	7.9	8.6
B-16	KP-23	26.51-26.53	8.5	7.8	8.5
B-17	KP-27	29.84-29.86	10.0	6.2	10.3
B-18	KP-27	29.86-29.86	13.0	8.7	11.9
B-19	KP-28	21.94-21.96	9.8	6.7	8.6
B-20	KP-27	11.27-11.29	9.9	9.5	9.6
B-21	KP-23	16.74-16.76	9.6	3.0	8.3
B-22	KP-27	22.24-22.25	7.8	8.6	7.1
B-23	KP-28	22.13-22.15	8.6	5.9	7.3
B-24	KP-28	32.89-32.91	9.2	6.4	9.8
B-25	KP-28	16.40-16.42	7.7	6.3	7.8
B-26	KP-23	21.44-21.46	10.9	6.3	10.6
B-27	KP-23	21.35-21.37	-	-	-
B-28	KP-16	25.09-25.11	7.2	7.8	6.9
B-29	KP-15	56.28-56.30	8.7	10.0	6.9
B-30	KP-16	25.19-25.21	7.0	8.1	6.6
B-31	KP-16	25.21-25.23	6.9	7.3	5.9
B-32	KP-16	25.23-25.25	6.5	7.0	4.2
B-33	KP-16	23.71-23.74	5.1	7.0	5.3

Table 2.1 Brazilian tensile test data - test results

and t is the thickness of the disc. Indirect tensile strength is plotted against percent TOC and X-ray maximum intensity ratio of quartz (I_Q) and illite (I_I) on figures 2.1 and 2.2 respectively. Linear regression gave the following results:

$$\sigma_t = 11.8 - 0.35(TOC) \qquad (MPA) \tag{5}$$

$$n = 32$$

$$r^2 = 0.067 \quad (\alpha > .50, \text{ i.e. random})$$

$$\sigma_t = 2.19 + 0.82(I_Q/I_I) \qquad (MPa) \tag{6}$$

$$n = 32$$

$$r^2 = 0.750 \quad (\alpha < .0001)$$

where α is the probability of the correlation having been generated randomly. The tensile strength is influenced significantly by the mineral matter and to a much lesser degree by the organic content. Moisture conditions of the samples were consistent with water contents ranging from 0.7 - 2.2 %. The data indicate that variations in moisture content had no effect whatsoever on the results, although this hypothesis cannot be subjected to rigorous statistical tests, because of the extremely narrow range of values.

The regression fit obtained by using the X-ray maximum intensity ratio of the quartz and illite peaks is quite similar to regression fits obtained for the Green River Formation where volumetric organic content (%Oc) is used, rather than mineral content, as the main controlling factor on rock strength. There are two factors which must be assessed in explaining the lack of a significant relationship to TOC. First, the range of TOC values tested in the provided samples is small. Maximum range is from 0% - 20% Oc for the Kettle Point Formation against 0% - 60% Oc for the Green River Formation. Second, there is a fundamental difference between the Kettle Point Forma-

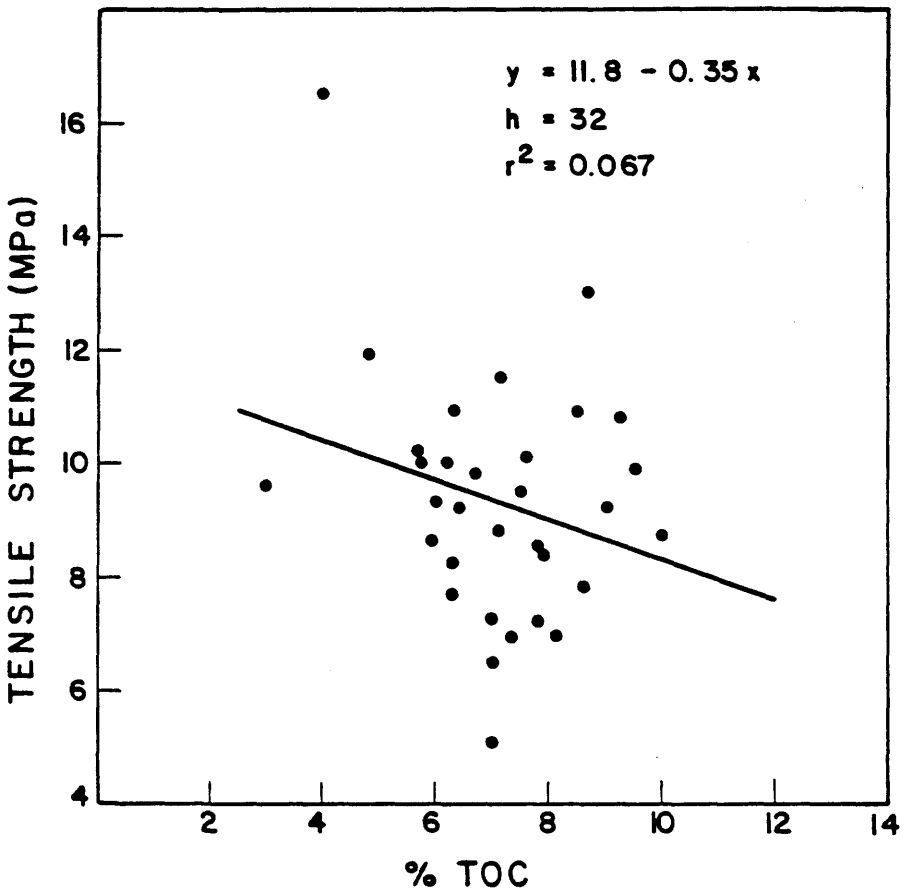

Figure 2.1 Brazilian tensile strength versus percent TOC

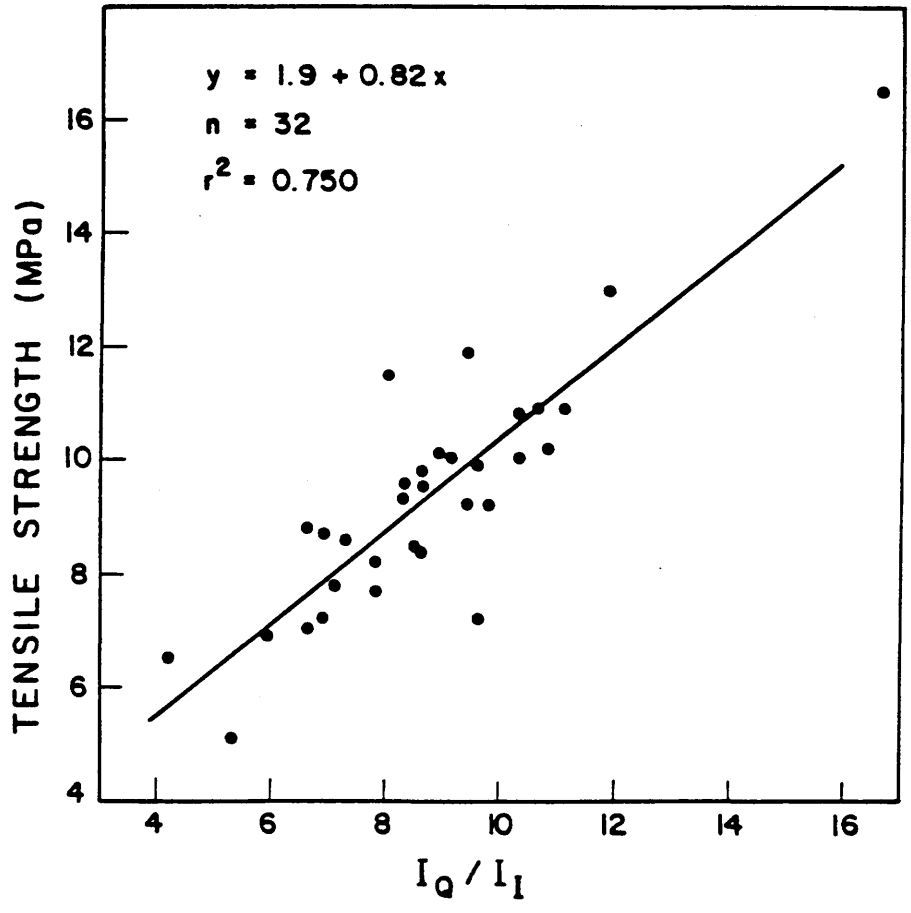

Figure 2.2 Brazilian tensile strength versus the X-ray maximum intensity ratio of quartz and illite.

tion and the well-tested Green River Formation. The former are matrix supported shales: that is, the mineral grains form the direct rock skeleton and the organic matter occurs mainly in the interstices, as coatings, or as inactive grains. The Green River shales are different: for very low-grade oil shale, carbonate minerals provide a structural matrix, but at higher grades the organic matter dilutes and weakens that support and has a dramatic effect on behavioral characteristics.

2.3 Uniaxial Compressive Test Data

2.3.1. Sample preparation and test procedure.

For sample preparation, ISRM suggested methods were used as a guideline (Bieniawski et al., 1978). Samples were cut from the provided cores at a height to diameter ratio of 2 to 3. Sample ends were ground flat and parallel to within 0.002 radians and sample dimensions were measured to the nearest 0.1 mm and recorded along with a brief sample description.

Due to the inherent weakness of the bedding planes, many samples broke during the cutting and grinding procedure and were set aside for other use. This bedding plane weakness is, as mentioned earlier, one of the characteristics of the Kettle Point Formation which causes great difficulties in sample preparation. The samples had to be treated with great care and it proved necessary to minimize the use of water in cutting and grinding procedures. If water had to be used, only the area to be cut or ground was exposed to the water and the rest of the sample covered by plastic wrap.

Strain gauges were attached to all samples to monitor stress versus strain relationships over the central zone of the specimens, to estimate Pois-

son's Ratio, and to compare strain gauge readings with overall axial displacement measurements monitored by LVDT and recorded on a chart recorder. For some samples, two different sizes of strain gauges, small and large, were used to investigate possible effects of the gauge length on strain resolution. The testing was performed using a stiff servo-controlled hydraulic loading system in a 500 tonne loading frame. Rate of loading was displacement controlled at approximately 5×10^{-6} sec^{-1} (5×10^{-5} cm/sec). Time to failure for specimens averaged 3000 sec, corresponding to an average failure strain of 1.5%.

2.3.2 Test results

Results are tabulated in table 2.2 and stress versus strain diagrams for all the samples are given on figures 2.3 to 2.8. As can be seen on the figures, the shape and slope of the stress/strain curves monitored by strain gauges or by axial LVDT measurements are quite different, particularly in the early stage of testing. The high strains at the beginning of each test, as monitored by axial LVDT measurements, cannot be explained solely in terms of microcrack closure. Initial seating effects at platen contact surfaces and alignment of the sample, platens, and loading ram all contribute to this non-linearity. Non-parallelism of sample ends, different deformation characteristics of individual layers within the rock sample, strains in the loading device, along with seating and alignment problems, are the causes of differences in the modulus values. The offset strain (ε_o) which is an indirect measure of non-linear ductility (figure 2.3), is very similar in axial LVDT and strain gauge measurements. On figure 2.9, the modulus of deformation (Young's modulus) obtained through strain gauge measurements over the central zone of the sample is plotted against the same parameter obtained through LVDT

SAMPLE NO	BOREHOLE	DEPTH (M)	σ_1 (MPa)	E_{GAUGE} (GPa)	E_{LVDT} (GPa)	ν	%TOC	I_Q/I_I
UN-1	KP-28	21.85-21.96	83.9	8.7[1]	6.2	0.226	8.0	8.6
UN-2	KP-27	11.13-11.25	99.6	10.1[1]	7.2	0.262	9.3	9.9
UN-3	KP-16	62.56-62.67	89.6	10.1[1]	6.5	0.220	6.4	10.2
"	"	" "	"	9.0[2]	"	"	"	"
UN-4	KP-16	23.74-23.84	58.9	5.9[1]	4.5	0.285	8.2	6.5
"	"	" "	"	6.5[2]	"	"	"	"
UN-5	KP-27	18.13-18.25	88.6	8.8[2]	6.2	0.194	10.3	7.2
UN-6	KP-20	19.30-19.40	75.9	9.1[1]	5.6	0.239	4.5	7.4
"	"	" "	"	8.4[2]	"	"	"	"

1 = 5 mm gauge: 2 = 14 mm gauge

Table 2.2 Uniaxial compression test data - test results

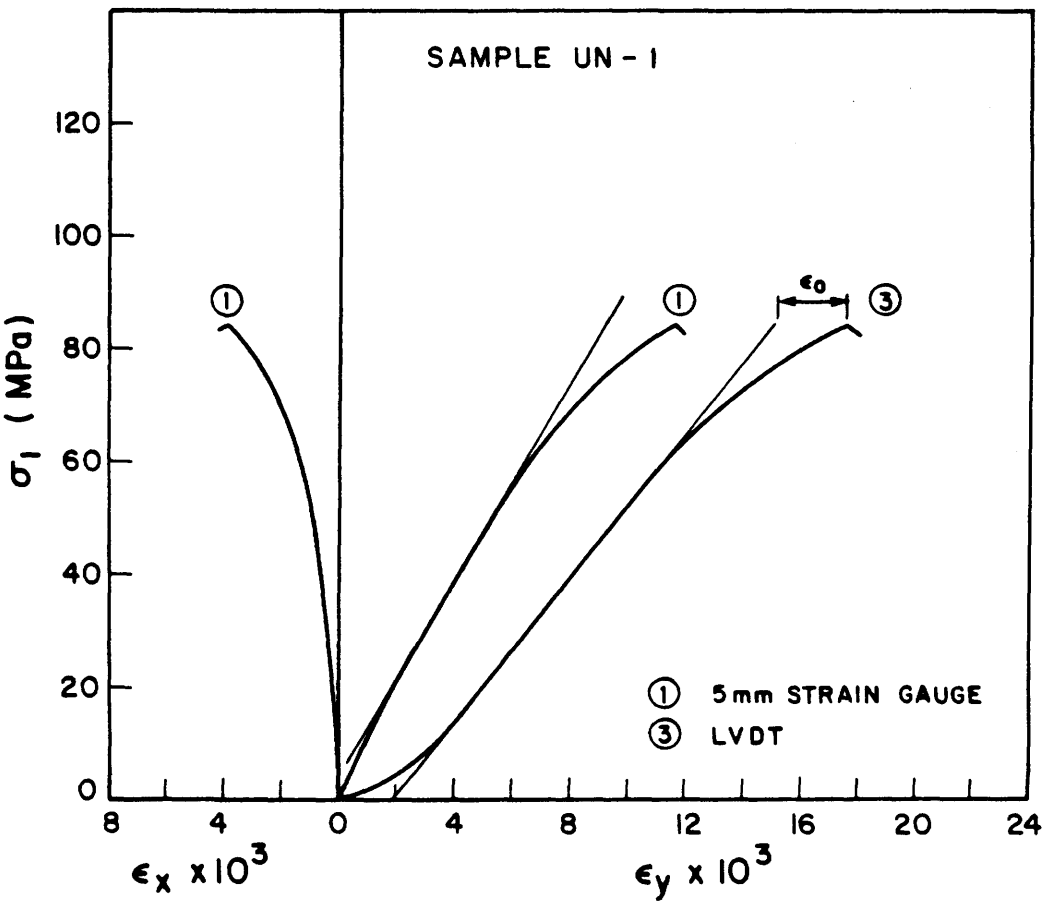

Figure 2.3 Stress versus strain relationship for sample UN-1.

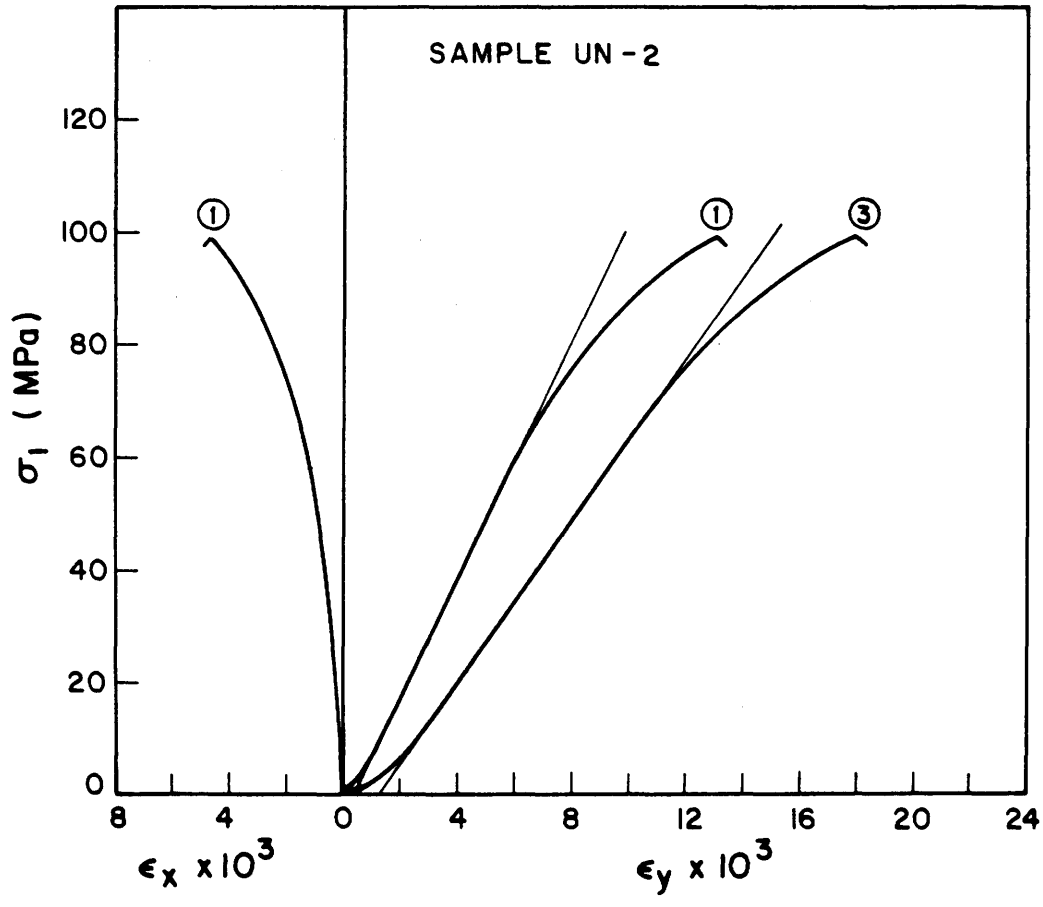

Figure 2.4 Stress versus strain relationship for sample UN-2.

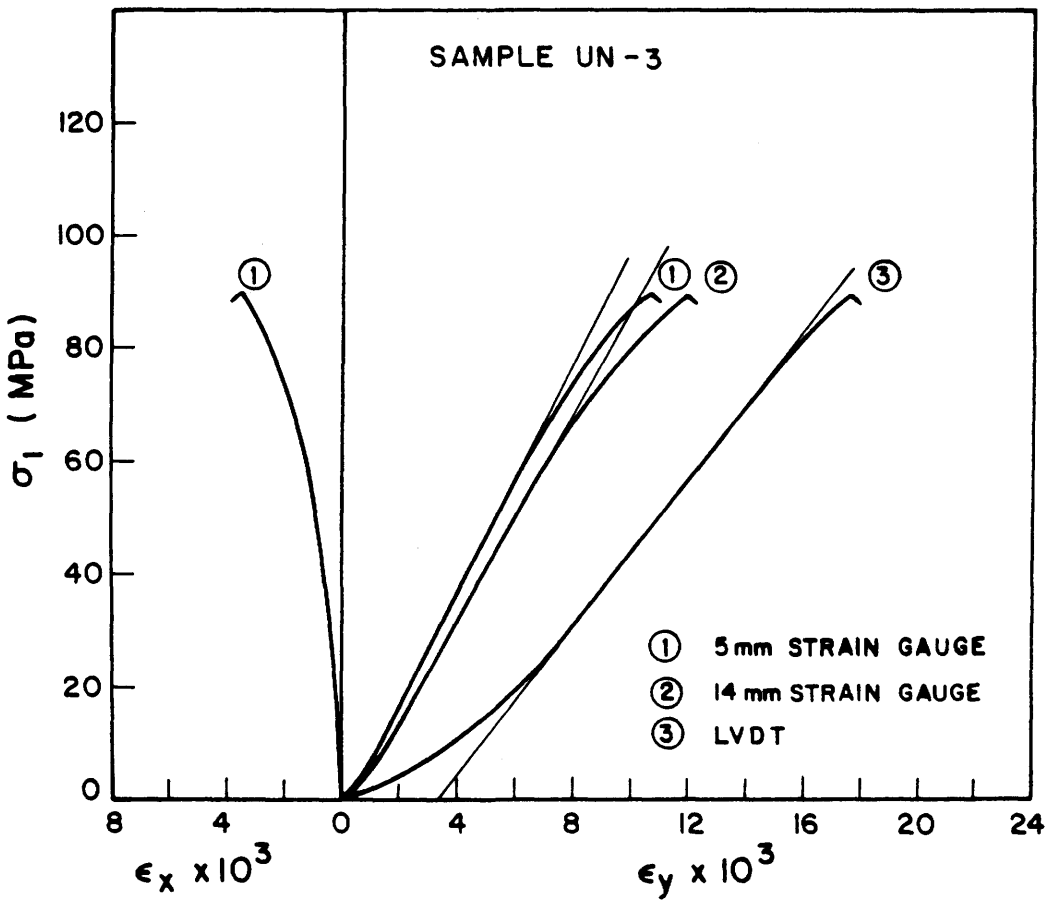

Figure 2.5 Stress versus strain relationship for sample UN-3.

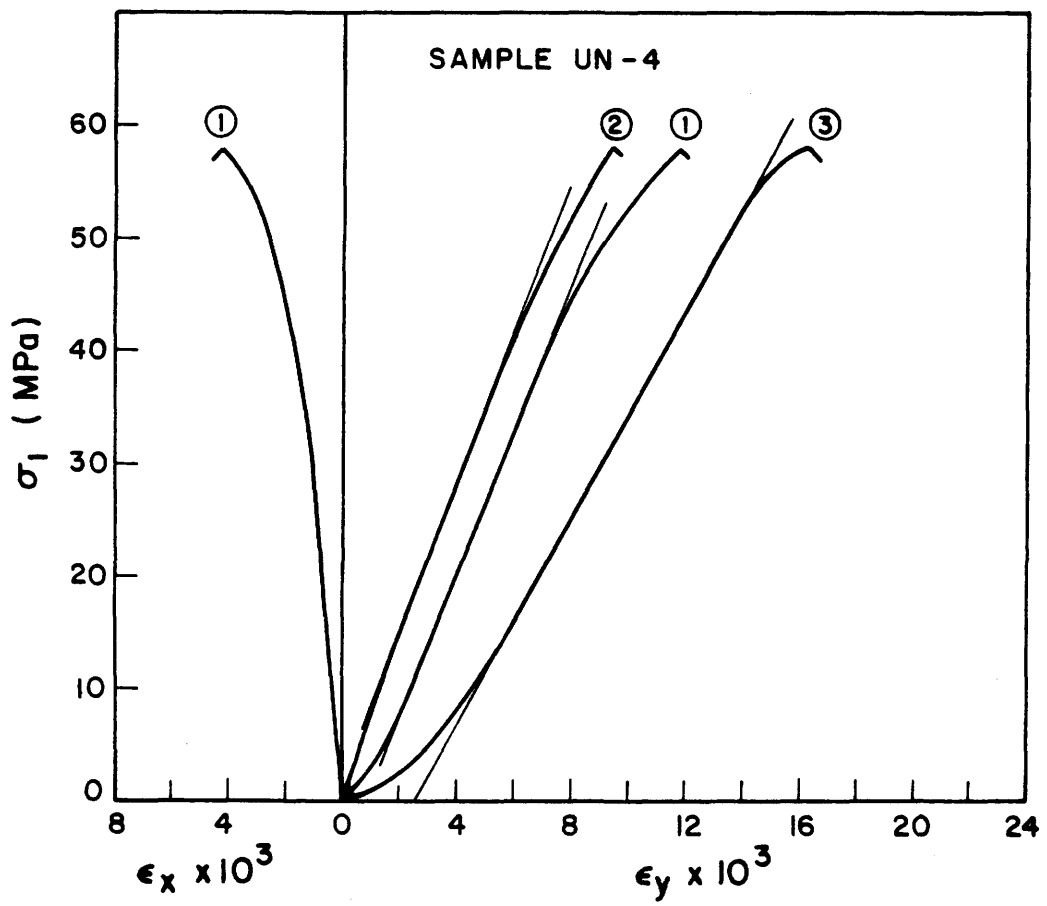

Figure 2.6 Stress versus strain relationship for sample UN-4.

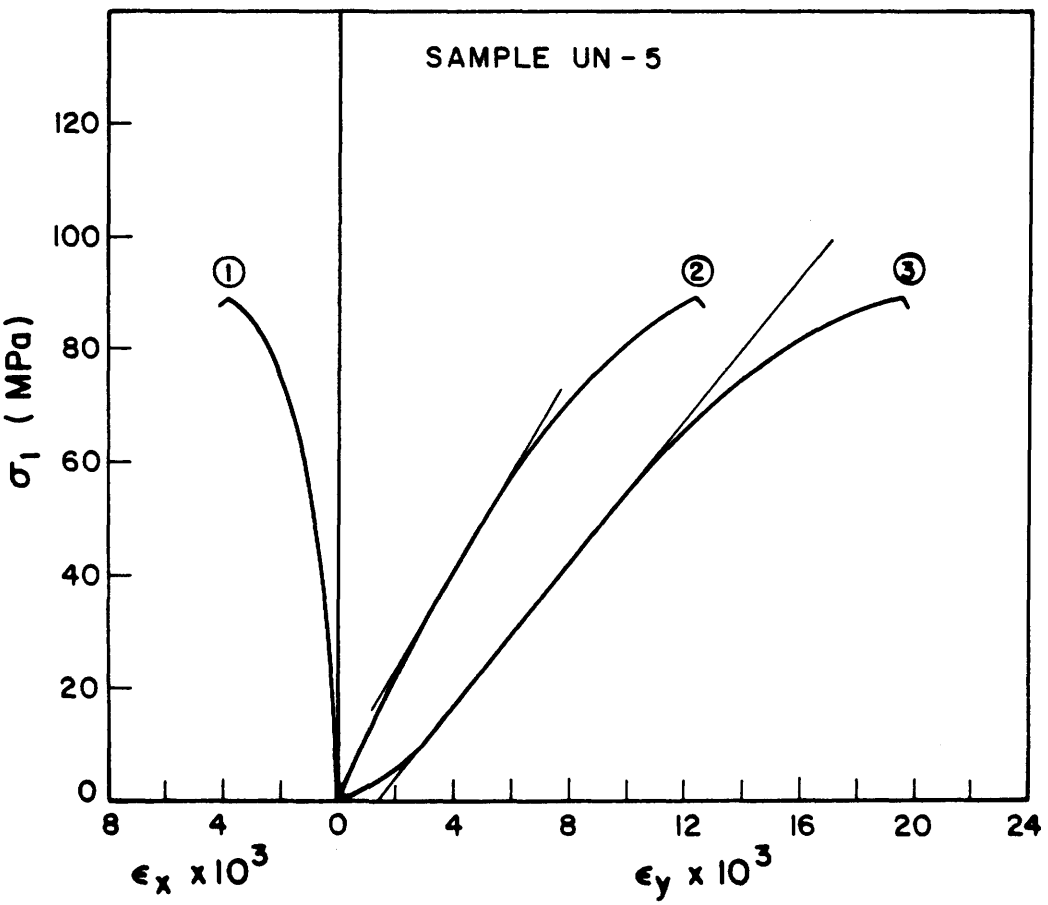

Figure 2.7 Stress versus strain relationship for sample UN-5.

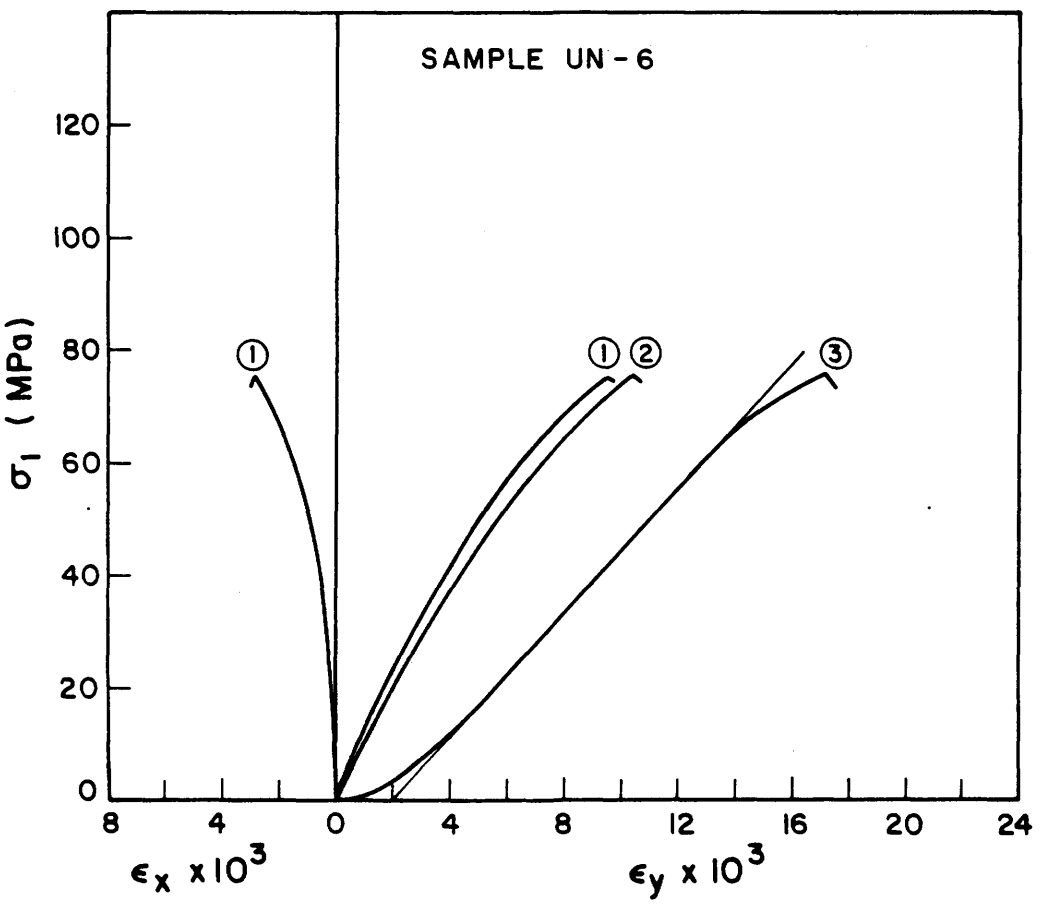

Figure 2.8 Stress versus strain relationship for sample UN-6.

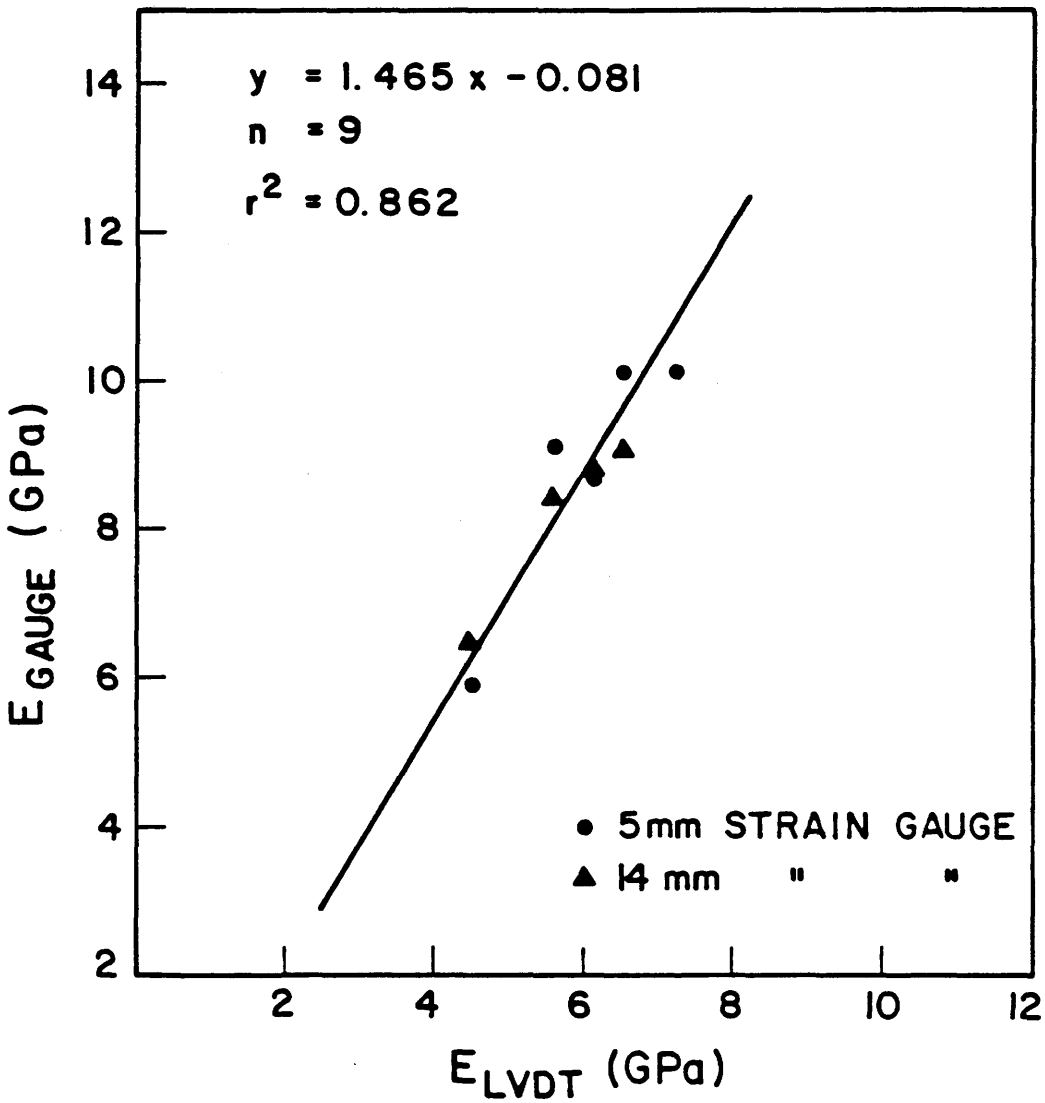

Figure 2.9 Modulus of deformation obtained through strain gauge measurements over the central zone of the samples versus the same parameter obtained through LVDT measurements of overall deformation.

measurements of overall deformation. Linear regression through all points gave the following results:

$$E_{GAUGE} = 1.465(E_{LVDT}) - 0.081 \quad (7)$$

$$n = 9$$

$$r^2 = 0.862 \quad (\alpha < 0.005)$$

The coefficient of determination (r^2) is high, indicating a consistent relationship. By forcing the regression line to go through zero, as one would expect for this case, the following expression is derived:

$$E_{GAUGE} = 1.45 * E_{LVDT} \quad (8)$$

that is, the modulus of deformation is about 45% greater in strain gauge measurements than obtained by overall axial LVDT measurements. The LVDT measurements in this case are corrected for calculated strains in end platens and loading ram assuming linear elasticity. Because of the internal consistency evidenced, the above expression can be used to reasonably estimate the 'gauge modulus' for samples tested in triaxial compression where only overall axial LVDT deformation measurements are made. The use of longer strain gauges did give more representative results because of the heterogeneity and variation of the elastic properties between individual layers within the sample domain.

Uniaxial compressive strength, like Brazilian tensile strength, and for same reasons, is mainly influenced by the mineral content and not (or to a much lesser degree) by the organic content. Regression analyses using the X-ray mineralogy gave the following results:

$$\sigma_u = 23.0 + 7.20(I_Q/I_I) \quad (9)$$

$$n = 6$$

$$r^2 = 0.609 \quad (\alpha = 0.11)$$

The r^2 value of 0.61 does not meet 95% confidence limits (r^2 0.729 for N = 6). However, the r^2 value using TOC is 0.01 ($\alpha > .999$). Because all other relationships in this study, for many tests, show the same direction of correlation, the relationship cannot be rejected as randomly generated. There is no doubt whatsoever that had more samples been tested, the 95% confidence criterion would have been met: all other factors indicate this.

Similarly, the modulus of deformation is influenced mainly by the mineral matter and not organic content. Linear regression gave the following results:

$$E_{LVDT} = 1.9 + 0.50(I_Q/I_I) \quad (10)$$

$$n = 6$$

$$r^2 = 0.693 \quad (\alpha = 0.06)$$

The corrected modulus for strain gauge measurements would be 45% greater or:

$$E_{GAUGE} = 2.7 + 0.73(I_Q/I_I) \quad (11)$$

Poisson's ratio, however, is not sensitive to the mineral ratio of quartz and illite. On other figures the uniaxial compressive strength, $(\sigma_1 - \sigma_3)/2$ for σ_3 = 0.0, and modulus of deformation are plotted along with the data obtained in triaxial testing.

2.4 Triaxial Compression Test Data

2.4.1 Sample preparation and test procedure

For sample preparation, ISRM suggested methods were used as a guideline and are basically the same as for preparation of samples for uniaxial compression test (Vogler and Kovari, 1977). In addition to the grinding of the ends of each specimen, the sides were ground and smoothed to ease the

placement of the samples in the triaxial cell. No strain gauges were attached to the sample, and stress versus overall displacement was monitored on a chart recorder. The rate of loading was the same as for uniaxial compression tests, i. e. a strain rate of approximately 5×10^{-6} sec^{-1}, and the testing was performed using the same loading system. The confining pressure was applied through an Enerpac pump and, to control and maintain the correct pressure, data were continuously displayed on a digital pressure gauge connected to a pressure transducer. During the tests the confining pressure could be easily controlled to $\pm$ 70 KPa with this system, which is an error of less than 2.0%.

2.4.2 Test results

Results from the triaxial tests are tabulated in table 2.3 and stress versus strain relationships for all the tested specimens are graphically displayed on figures 2.10 to 2.16. On figure 2.17, $(\sigma_1 - \sigma_3)/2$ is plotted against $(\sigma_1 + \sigma_3)/2$ at failure (σ_{1p}) for all samples tested in uniaxial and triaxial compression. The fracture strength of a sample (σ_{1f}) is the ultimate frictional strength of a fracture created by loading an intact sample well past its peak strength. As seen on the figure, a failure envelope can not be designated by a single line, but rather as a zone bounded by upper and lower limits. These upper and lower boundaries could be drawn as regression lines through upper and lower data points, as shown on figure 2.17, but by examining the data more carefully, in context of the sample mineral composition, a different approach is warranted. As shown on figure 2.18, triaxial compression strength and uniaxial compression strength are closely related to the mineral ratio of quartz and illite as determined by intensity of X-ray peaks. Linear regression analyses of the data points on figure 2.18 gave the following results:

SAMPLE NO	BOREHOLE	DEPTH (M)	σ_{1p} (MPa)	σ_{1f} (MPa)	σ_3 (MPa)	E_{LVDT} (GPa)	%TOC	I_I/I_I
TR-1	KP-22	24.36-24.47	-	-	-	-	-	-
TR-2	KP-28	24.08-24.19	93.3	25.7	1.7	6.2	5.4	8.8
TR-3	KP-23	26.54-26.65	92.5	32.0	3.5	6.0	5.5	7.5
TR-4	KP-28	24.20-24.31	92.2	33.7	3.5	6.1	10.2	8.1
TR-5	KP-22	13.76-17.88	85.3	27.9	3.5	6.2	4.6	7.7
TR-6a	KP-23	26.38-26.49	114.6	-	13.8	6.3	8.9	7.7
TR-6b	KP-23	26.38-26.49	133.0	80.4	20.7	7.1	8.9	7.7
TR-7	KP-17	75.15-75.25	124.2	65.2	13.8	7.0	5.7	8.3
TR-8	KP-22	24.21-24.32	145.9	75.5	13.8	8.2	7.6	10.3
TR-9	KP-28	16.20-16.30	106.2	59.6	13.8	6.2	3.4	7.3
TR-10	KP-27	26.54-26.65	135.1	69.5	13.8	7.4	10.2	8.7
TR-11	KP-26	37.29-37.40	163.6	91.2	20.7	7.8	8.2	9.7
TR-12	KP-29	26.80-26.91	127.2	78.8	20.7	6.2	8.4	7.3
TR-13	KP-28	14.25-14.36	125.6	73.4	20.7	6.4	9.4	7.2
TR-14	KP-25	41.71-41.82	118.0	75.3	20.7	5.9	9.5	7.7

Table 2.3 Triaxial compression test data - test results.

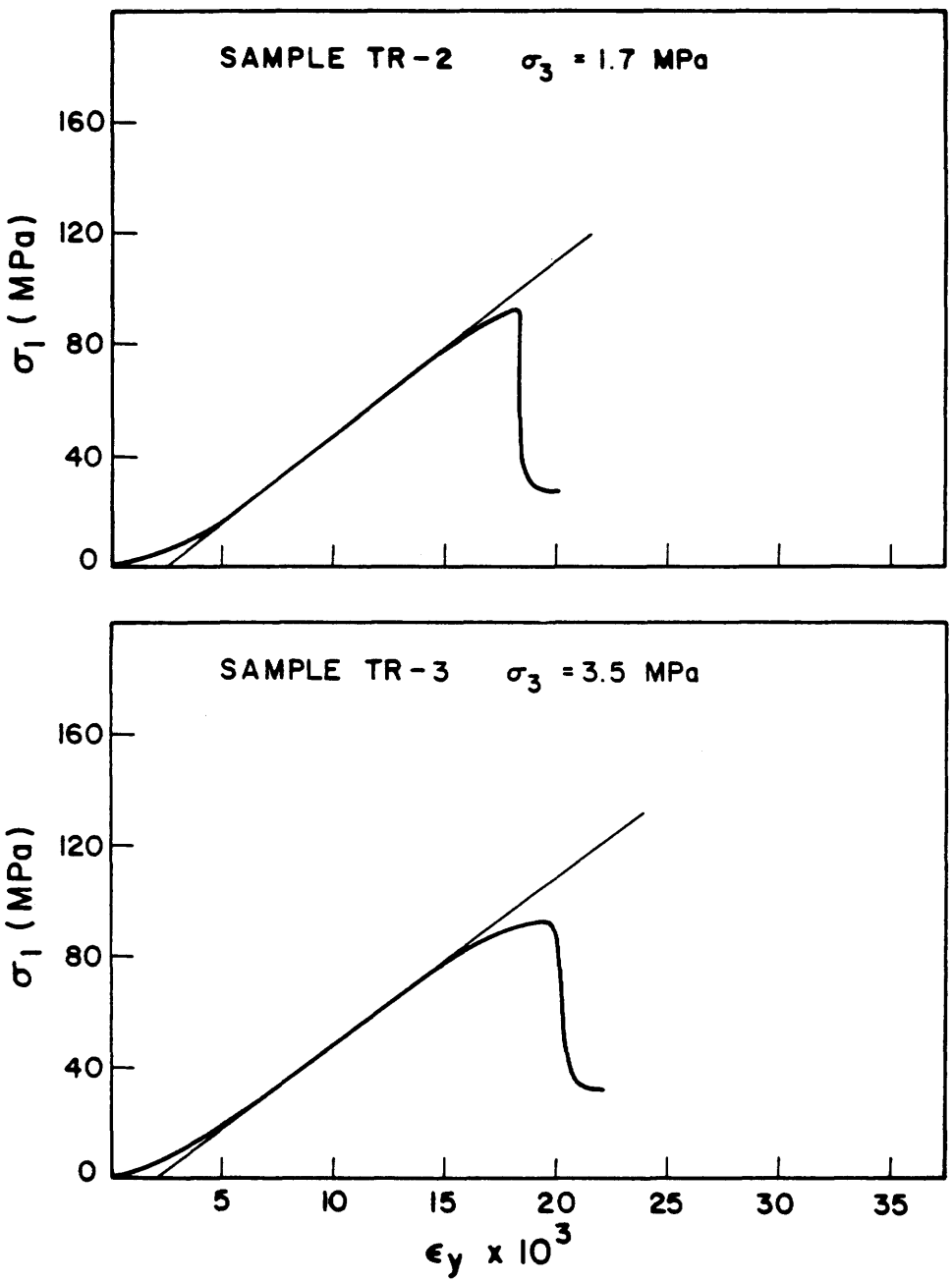

Figure 2.10 Stress versus strain curves for samples TR-2 and TR-3.

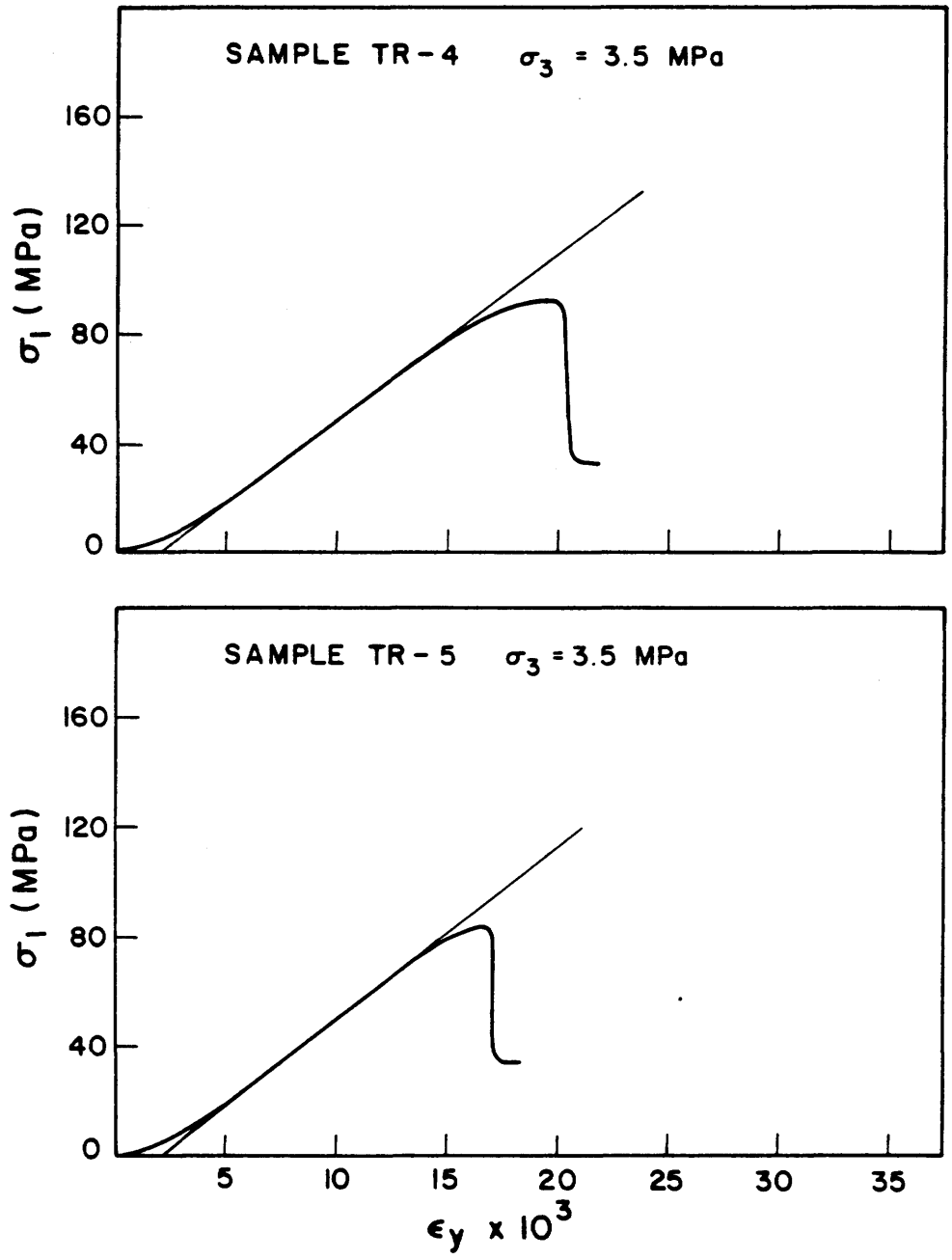

Figure 2.11 Stress versus strain curves for samples TR-4 and TR-5.

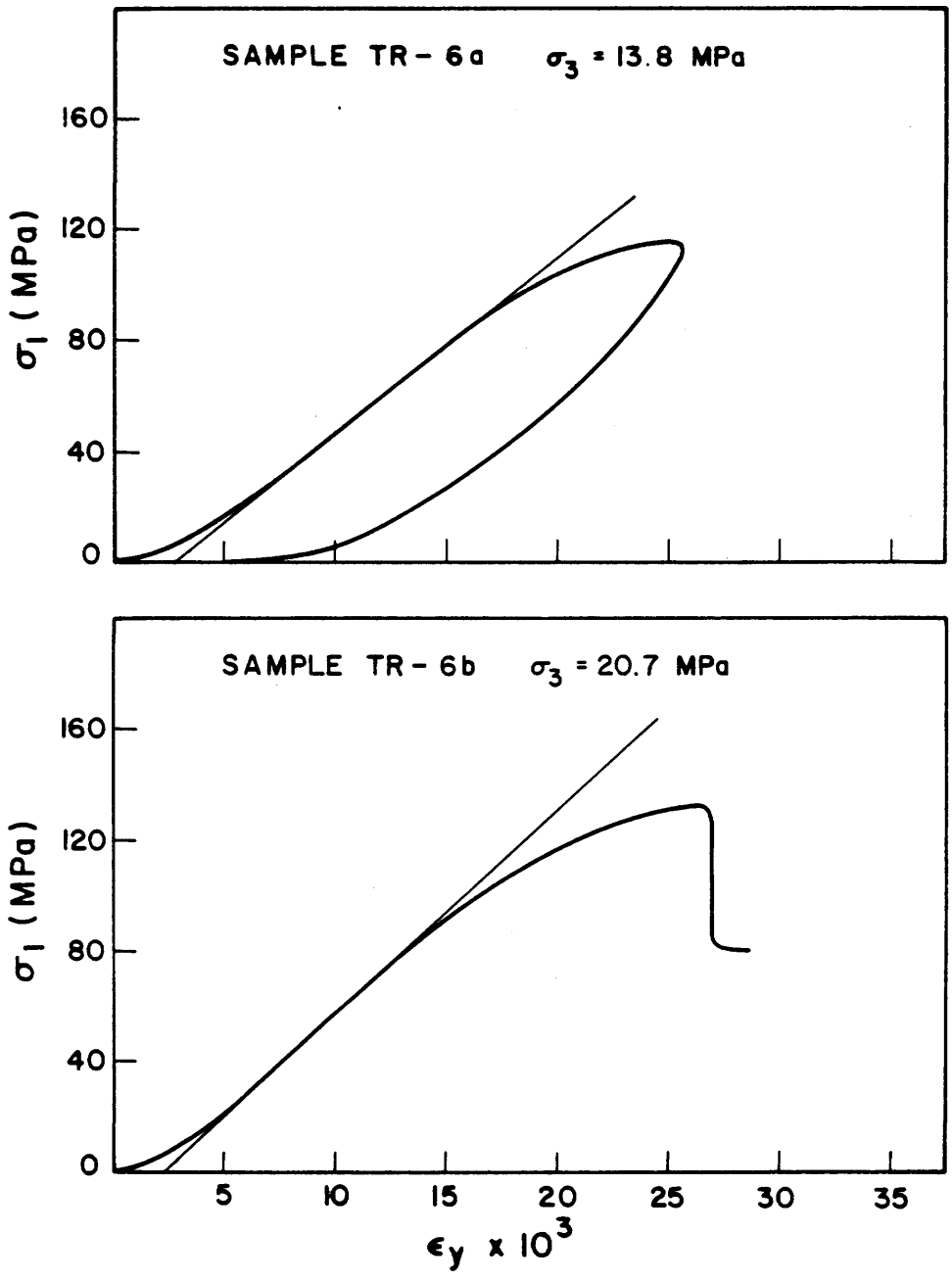

Figure 2.12 Stress versus strain curves for samples TR-6a and TR-6b.

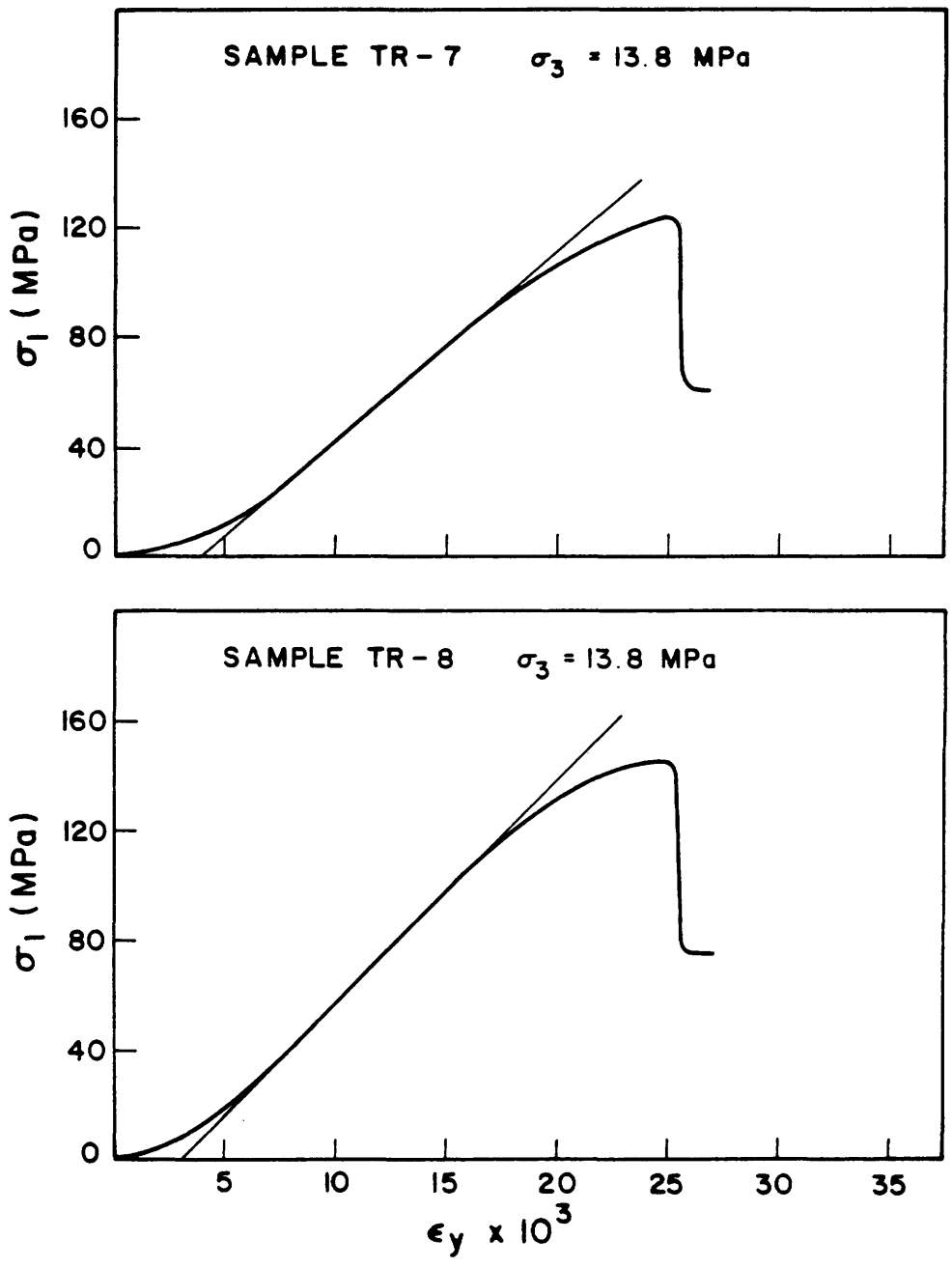

Figure 2.13 Stress versus strain curves for samples TR-7 and TR-8.

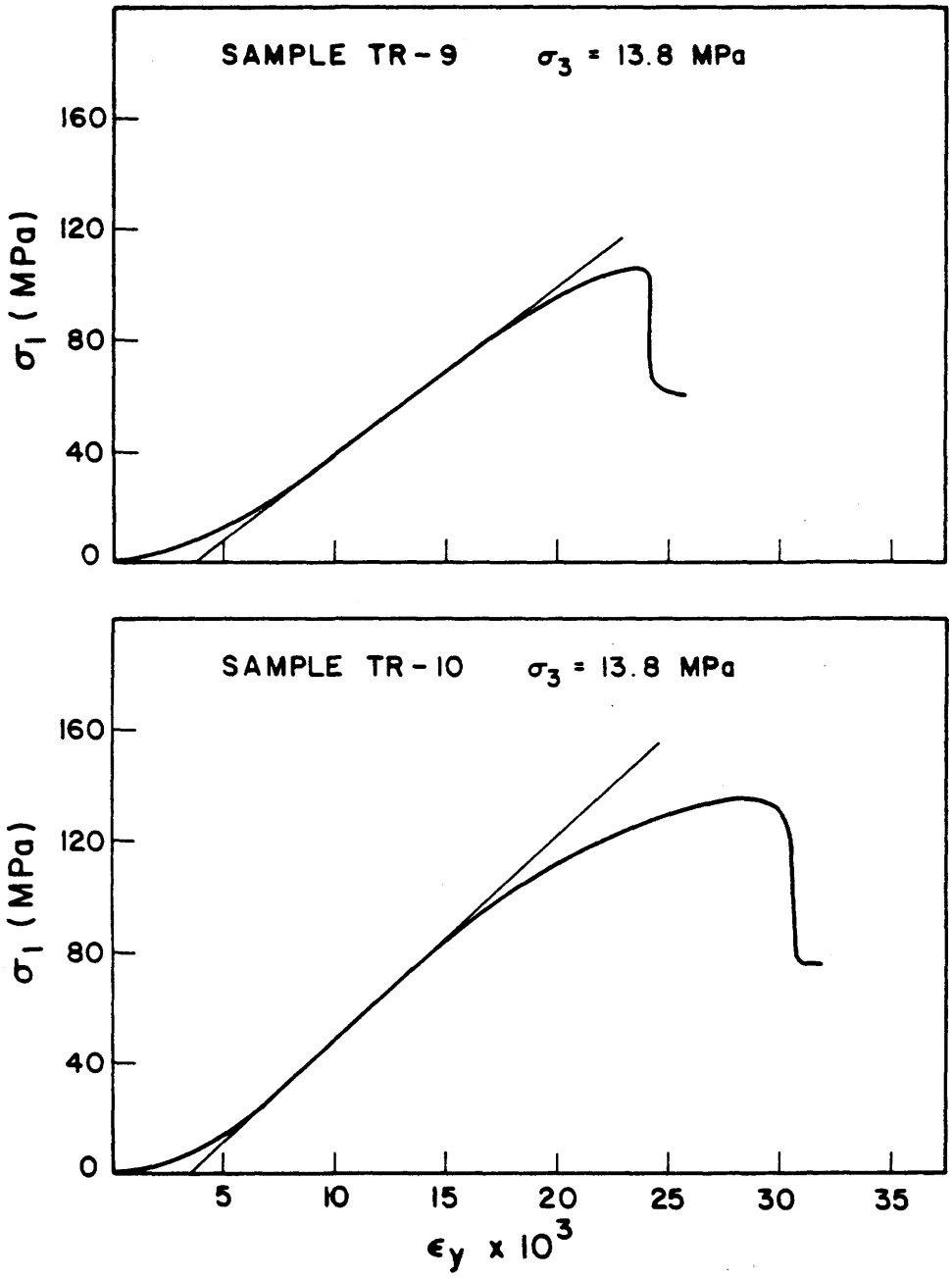

Figure 2.14 Stress versus strain curves for samples TR-9 and TR-10.

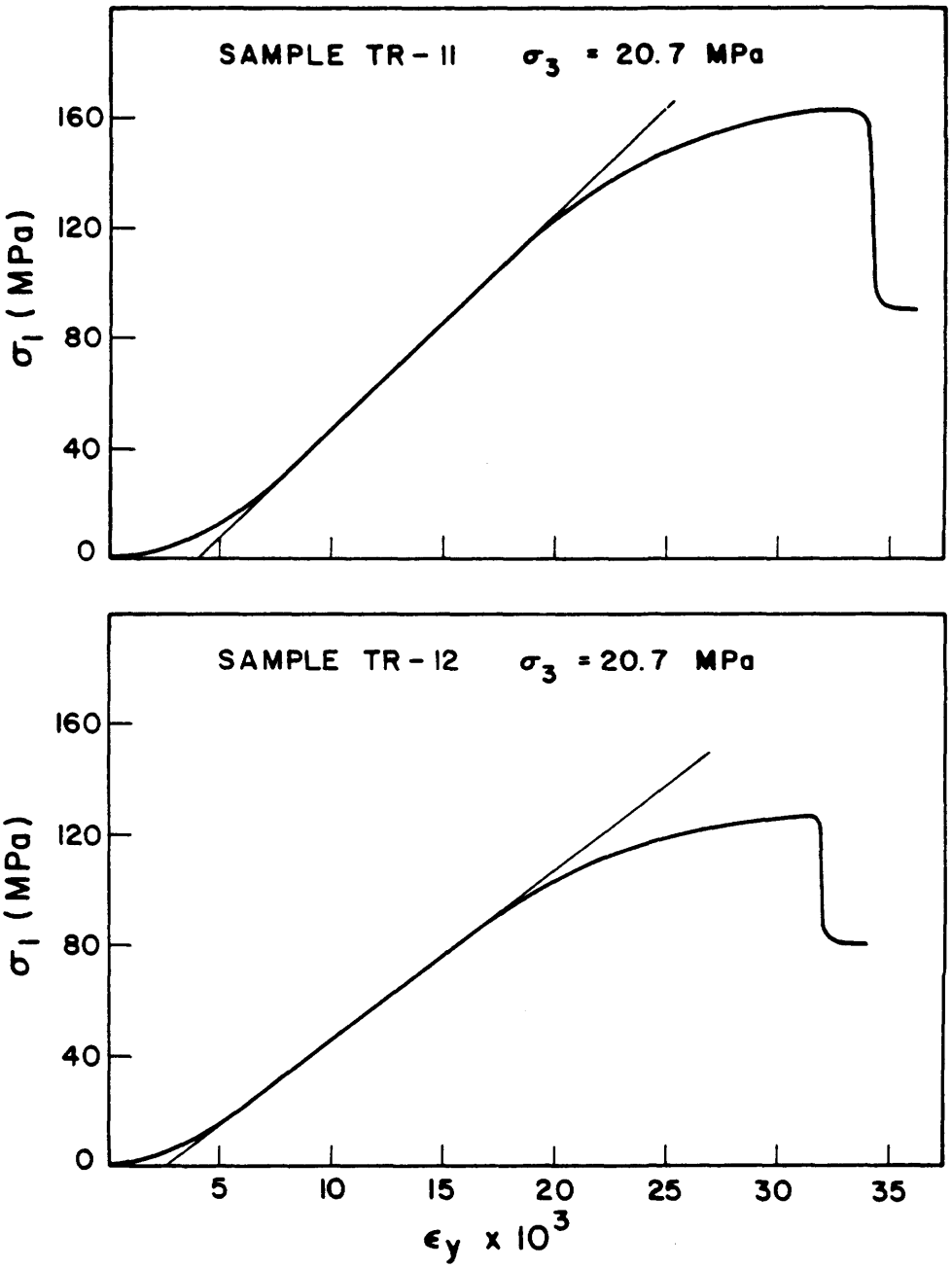

Figure 2.15 Stress versus strain curves for samples TR-11 and TR-12.

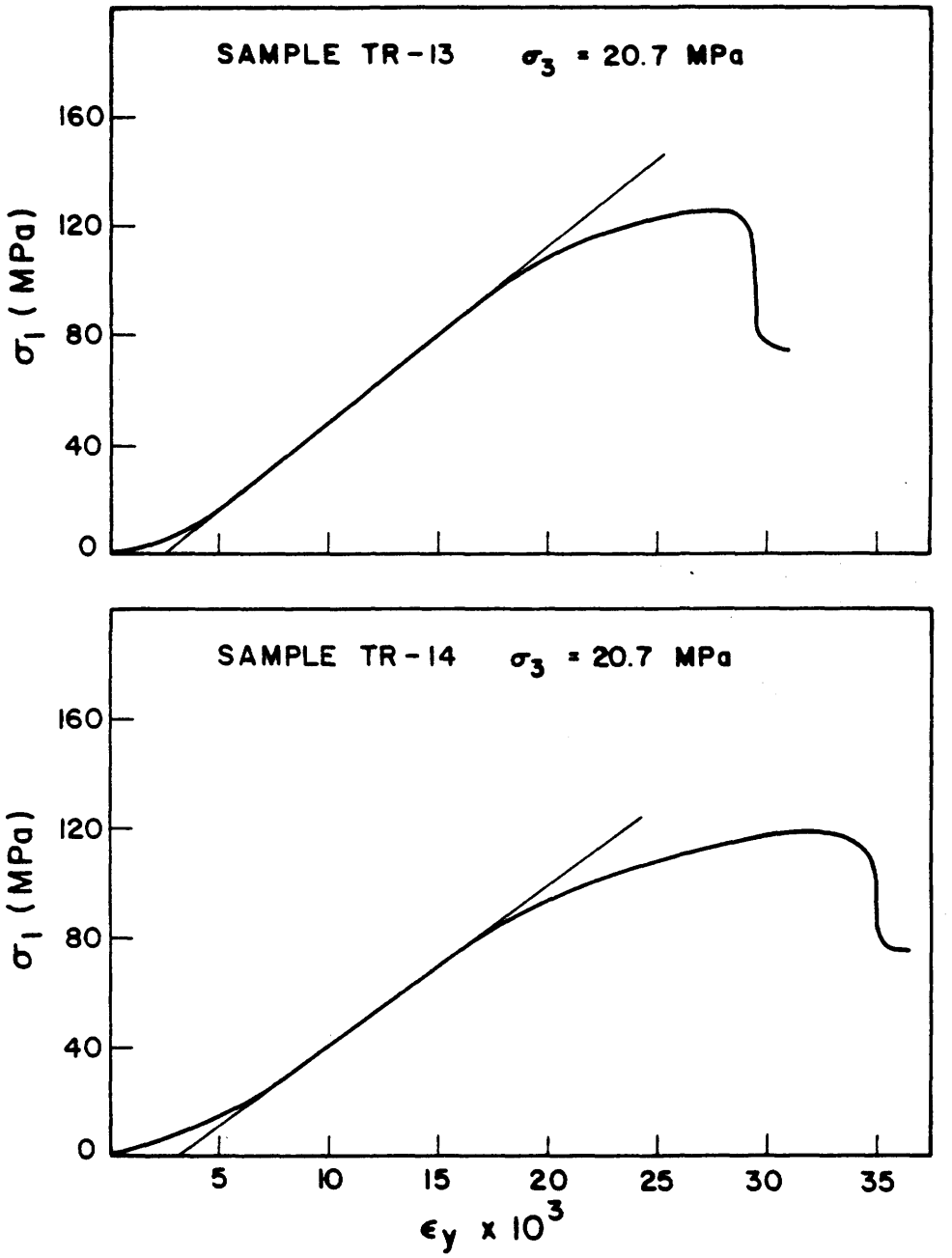

Figure 2.16 Stress versus strain curves for samples TR-13 and TR-14.

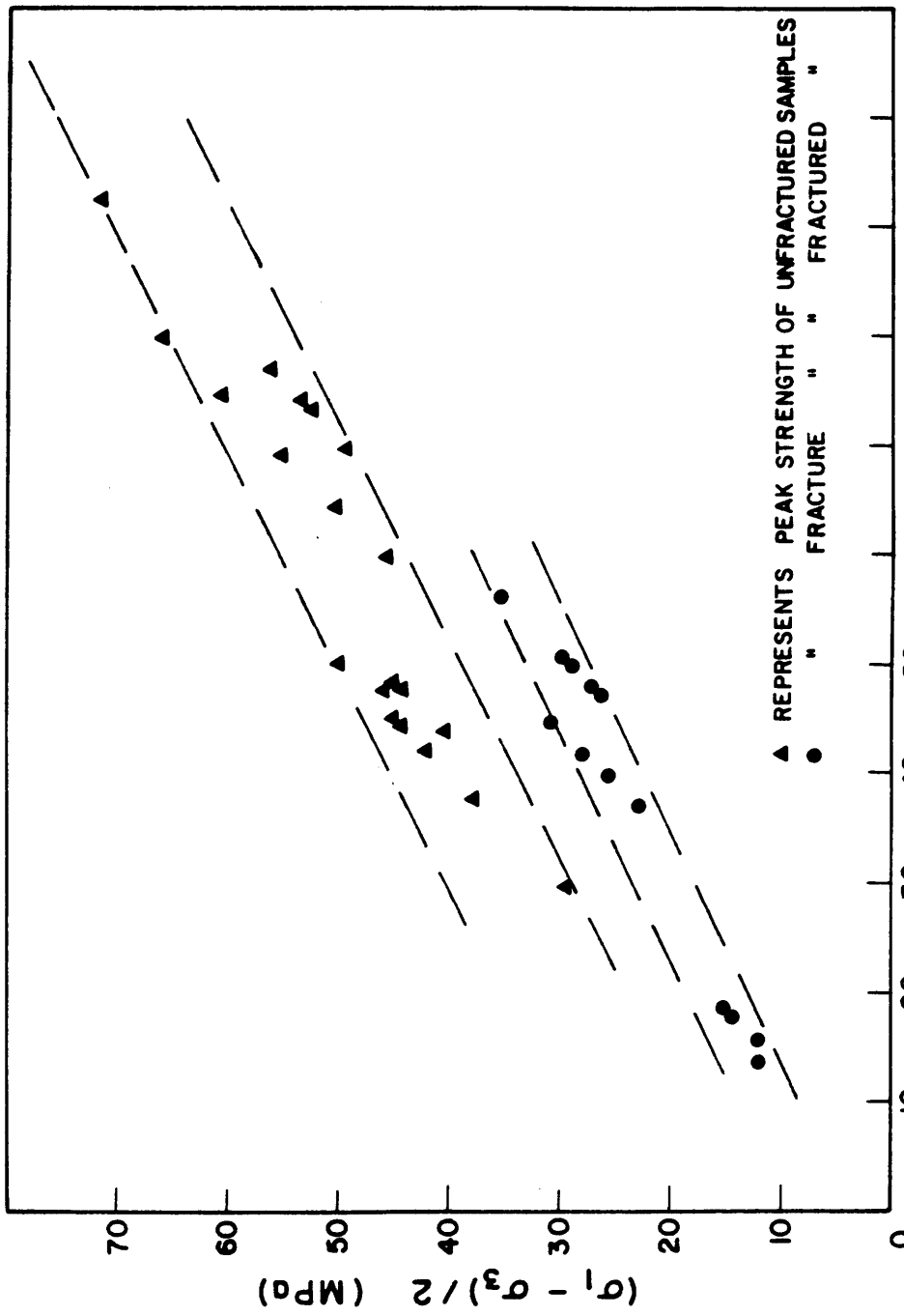

Figure 2.17 $(\sigma_1-\sigma_3)/2$ versus $(\sigma_1+\sigma_3)/2$ diagram with upper and lower boundaries.

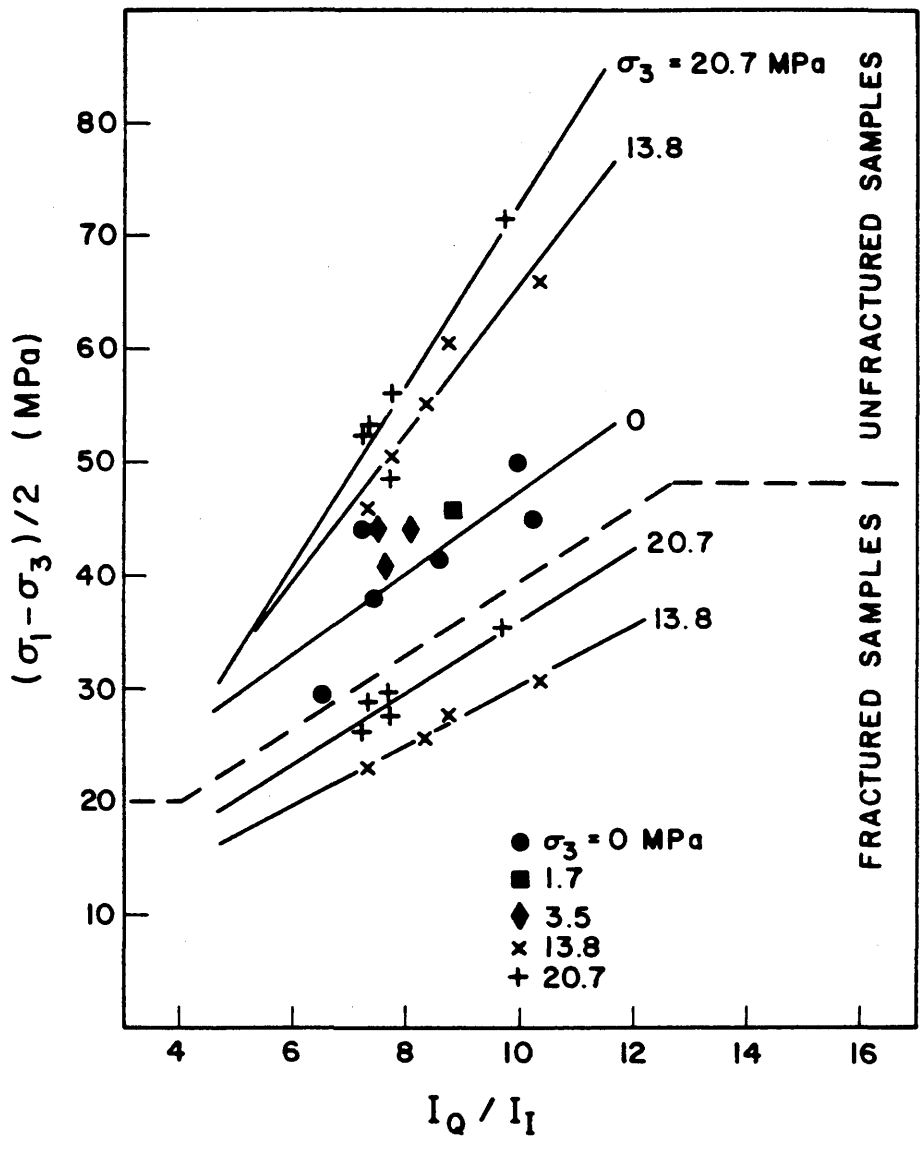

Figure 2.18 $(\sigma_1-\sigma_3)/2$ versus the maximum intensity ratio of quartz and illite.

$$(\sigma_{1p}-\sigma_3)/2 = 11.5 + 3.60(I_Q/I_I) \quad \text{(MPa)} \tag{12}$$

σ_3 = 0.0 MPa

n = 6

r^2 = 0.609 (same data as eqn. 9, α = 0.11)

$$(\sigma_{1p}-\sigma_3)/2 = 0.2 + 6.56(I_Q/I_I) \quad \text{(MPa)} \tag{13}$$

σ_3 = 13.8 MPa

n = 5

r^2 = 0.927 (α = 0.01)

$$(\sigma_{1p}-\sigma_3)/2 = -7.0 + 8.00(I_Q/I_I) \quad \text{(MPa)} \tag{14}$$

σ_3 = 20.7 MPa

n = 5

r^2 = 0.855 (α = 0.04)

Despite small sample size and up to 10% observed errors in determination of the X-ray maximum intensity ratio of quartz and illite, are reasonably good. Furthermore, these regression analyses can be used to derive a failure criteria for all the samples as a function of the confining pressure (σ_3) and the intensity ratio of quartz and illite:

$$(\sigma_{1p}-\sigma_3)/2 = 21.0 + 0.059((\sigma_{1p}+\sigma_3)/2)(I_Q/I_I) \text{ (MPa)} \tag{15}$$

n = 20

r^2 = 0.949

As shown on figure 2.19 these results are different from the bounded zone on figure 2.17, indicating clearly the importance of determining the intrinsic material properties that influence the physical and mechanical characteristics of the material involved.

This correlation coefficient for n = 20 would imply an extremely high confidence value ($\alpha < 10^{-7}$), but it is not a valid statistical test because of

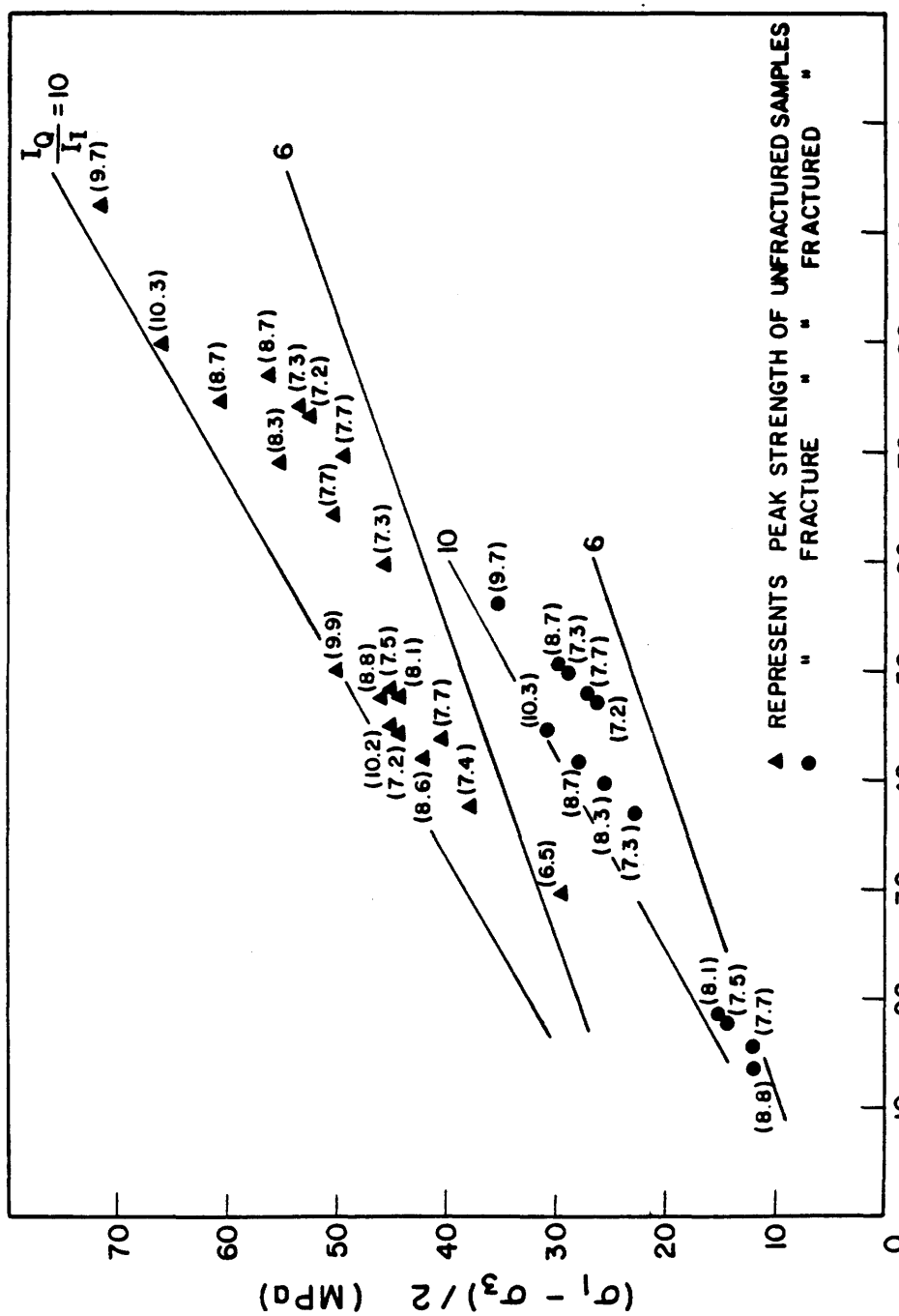

Figure 2.19 $(\sigma_1-\sigma_3)/2$ versus $(\sigma_1+\sigma_3)/2$ diagram with boundaries calculated according to equation 15. Figures in brackets are determined values of I_Q/I_I for each sample.

autocorrelation of the equation. The previous data (equation 12-14), however, show the effects of the independent variable, and permit the use of equation 15 at a confidence level of >95%. Since only the modified shear strength parameters a and @ are obtained from figure 2.19, the following equations must be used to convert a and @ to C (cohesion) and $\emptyset$ (intrinsic friction angle) respectively:

$$\emptyset = \sin^{-1}(\tan(@)) \tag{16}$$

$$C = a/\cos(\emptyset) \tag{17}$$

Furthermore, Mohr's coordinates for stresses acting on a failure surface can be obtained using the following transformation equations given by Franklin (1971):

$$\sigma n = (\sigma_1+\sigma_3)/2 - ((\sigma_1-\sigma_3)/2)(\tan(@)) = \text{normal stress} \tag{18}$$

$$T = (\sigma_1-\sigma_3)/2\sqrt{1 - \tan(@)^2} = \text{shear stress} \tag{19}$$

As previously defined, tan(@) is the slope of the failure envelopes on figure 2.19 and is approximately equal to $0.059(I_Q/I_I)$. On figure 2.20, failure envelopes calculated according to the above equations are compared to the Mohr-Coulomb criteria obtained by drawing a linear envelope touching the Mohr's principal stress circles. As can be seen on the figures, those are closely related.

Modulus of deformation in triaxial compression, as in uniaxial compression, is mainly influenced by the mineral matter and not organic content. Linear regression analyses gave the following results:

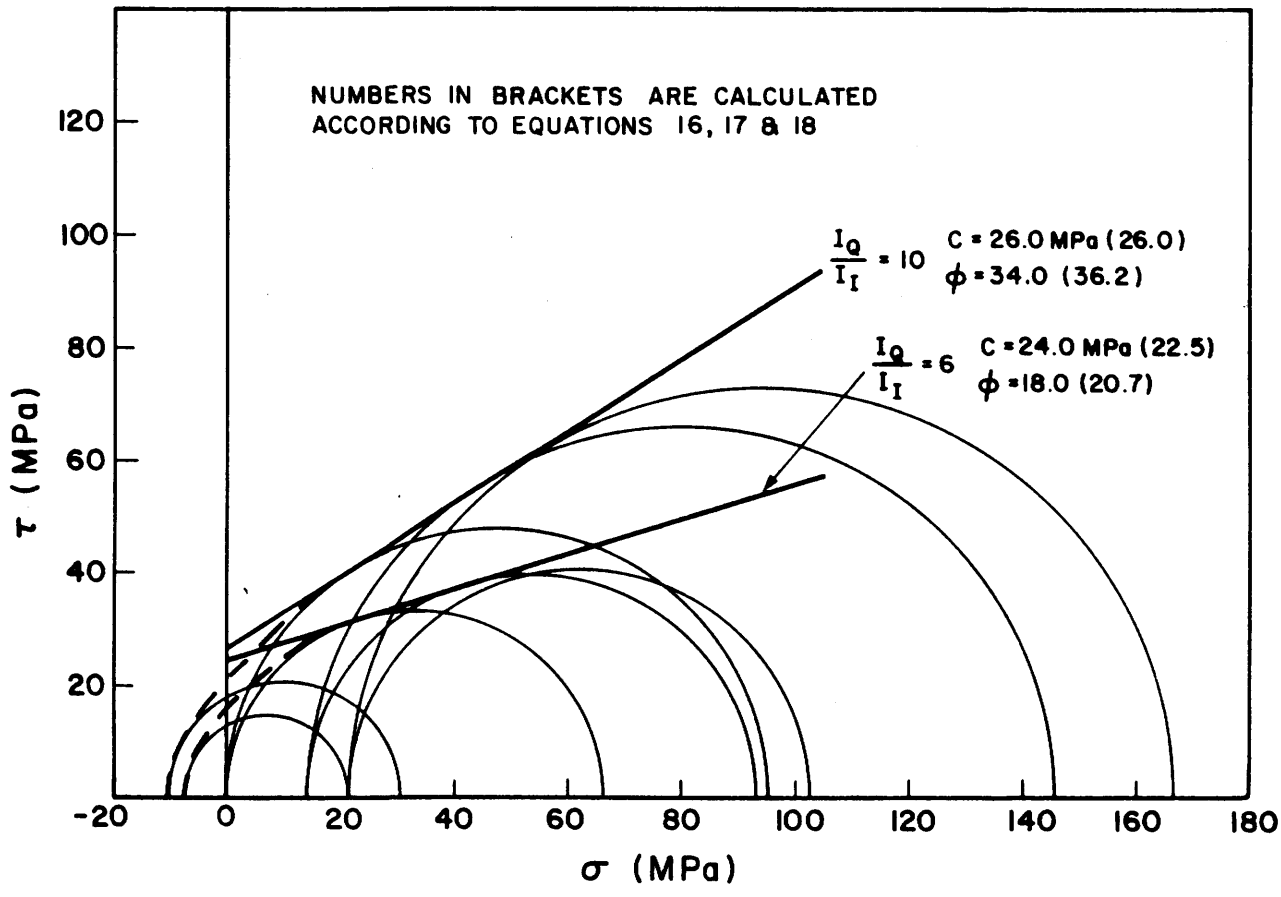

Figure 2.20 Comparison of the calculated values to the Mohr's-Coulomb failure envelope.

$$E_{LVDT} = 1.9 + 0.50(I_Q/I_I) \quad \text{(GPa)} \tag{20}$$

σ_3 = 0.0 MPa

n = 6

r^2 = 0.693 (same as eqation 10, α = 0.06)

$$E_{LVDT} = 1.1 + 0.70(I_Q/I_I) \quad \text{(GPa)} \tag{21}$$

σ_3 = 13.8 MPa

n = 5

r^2 = 0.963 (α = .005)

$$E_{LVDT} = 1.8 + 0.62(I_Q/I_I) \quad \text{(GPa)} \tag{22}$$

σ_3 = 20.7 MPa

n = 5

r^2 = 0.676

The similarity of these equations indicates that the deformation modulus is not influenced much by an increase in the confining pressure and the increase is no more than 10% - 15% as shown on figure 2.21. This is, however, not surprising for stiff strong material of low porosity (Lama and Vutukuri, 1978).

The ultimate frictional strength of fractures created by failing the samples in triaxial compression is not only highly influenced by the confining pressure but also the mineral ratio of quartz and illite. Samples that had high peak strengths had also high residual strength. Linear regression analyses yielded the following:

$$(\sigma_{1f}-\sigma_3)/2) = 3.9 + 2.65(I_Q/I_I) \quad \text{(MPa)} \tag{23}$$

σ_3 = 13.8 MPa

n = 4

r^2 = 0.968 (α = <0.6)

$$(\sigma_{1p}-\sigma_3)/2 = 4.5 + 3.16(I_Q/I_I) \quad \text{(MPa)} \tag{24}$$

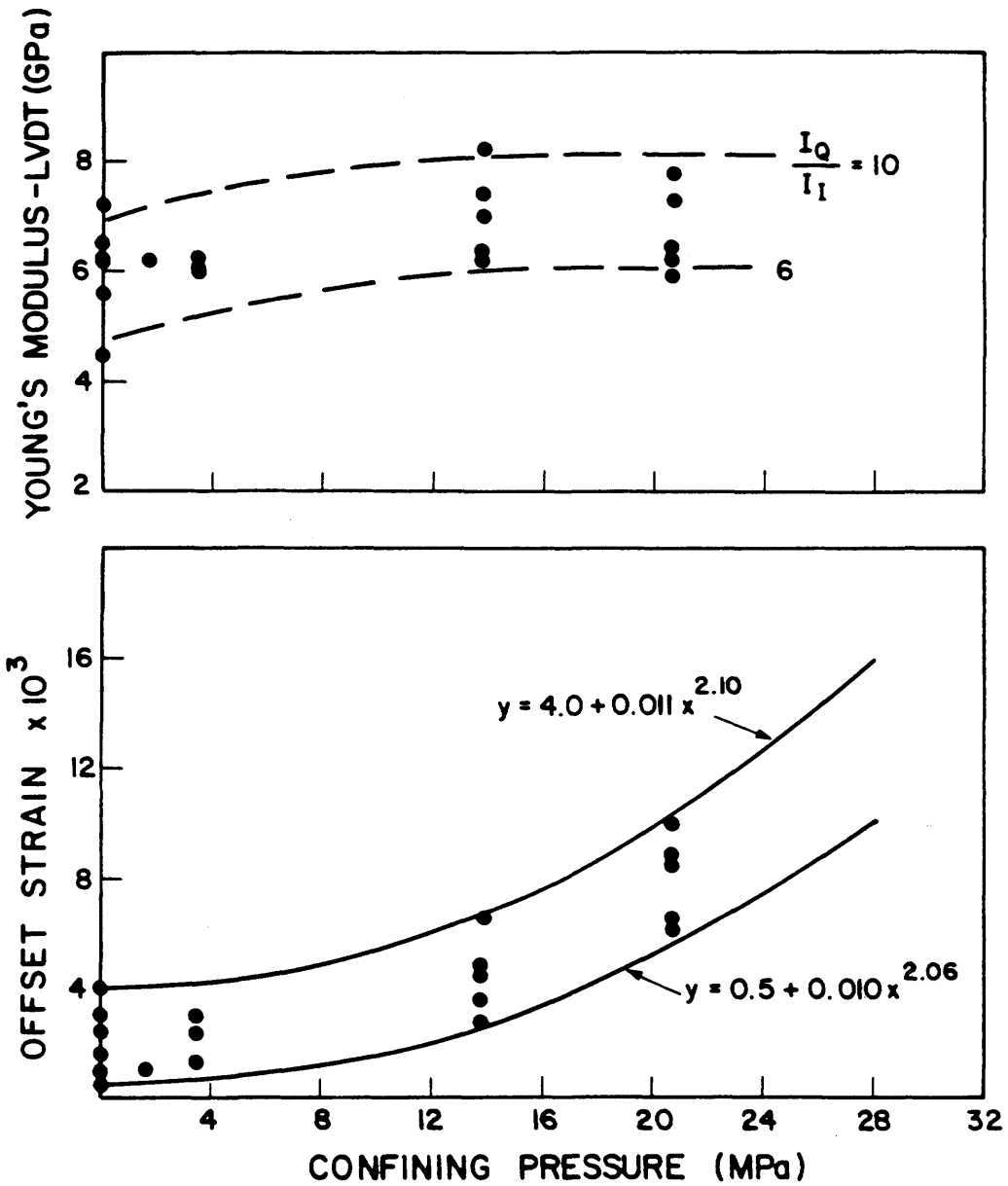

Figure 2.21 Young's modulus (LVDT) and offset strain versus the confining pressure.

σ_3 = 20.7 MPa

n = 5

r^2 = 0.867 (α = .03)

On figure 2.19 failure envelopes are drawn for the X-ray intensity ratios of 6 and 10. These envelopes are obtained from a three variable linear regression analysis of the composed data:

$$(\sigma_{1f}-\sigma_3)/2 = 6.6 + 0.056((\sigma_{1f}+\sigma_3)/2)(I_Q/I_I) \quad \text{(MPa)} \tag{25}$$

n = 13

r^2 = 0.974

The validity of this equation is limited at lower confining pressures since one would not expect high cohesive stresses to exist for open uncemented fractures. A more extensive data base may alter these relationships somewhat.

Ductility, or the deviation from linear elastic behavior, increases by increasing confining pressure, as expected. The amount of increase is not easily determined but an indirect estimate can be obtained by measuring the offset strain (figure 2.3). On figure 2.21, offset strain is plotted against confining pressure and it is apparent that ductile behavior becomes more and more dominant as the confinement increases. The offset strain is not a linear function of the confining pressure but rather it changes by a factor of σ_3^2 or (as shown on figure 2.21) according to the following equation:

$$\varepsilon_0 = (A + 0.01\sigma_3^{2,1})\times 10^{-3} \tag{26}$$

where $A \times 10^{-3}$ is the offset strain in uniaxial compression ranging from 0.5 $\times 10^{-3}$ to 4.0 $\times 10^{-3}$ for the samples tested in this investigation, and σ_3 is the confining pressure in MPa. Although failure envelopes on figure 2.19 are plotted as straight lines, results on figure 2.21 indicate that increasing deviations from linearity should be expected as the confinement increases. Further testing at higher confining pressures should confirm those deviations.

Linear regression analyses did not yield any acceptable functional relationship between offset strain and mineralogy or TOC contents. This is a reasonable result in the context of previous data.

2.5 Point Load Index Test Data

2.5.1 Sample preparation and test procedure

For sample preparation, suggested methods by Broch and Franklin (1972) were used as a guideline, with one exception. When loading perpendicular to bedding, at a height to diameter ratio of approximately unity, chipping usually occurred at one or both loading points instead of failure on a plane connecting the loading points. This chipping phenomenon was also observed by Kim (1978) and to avoid it sample height was reduced to approximately 1/2 the diameter. When loading parallel to bedding some samples failed without any appreciable load. This procedure was thus discontinued after a few tests. Dimensions of all samples were measured carefully and recorded along with sample descriptions.

2.5.2 Test results

Results are tabulated in table 2.4. The point load index was calculated using the equation presented by Broch and Franklin (1972):

$$Is = P/D^2 \qquad (27)$$

where Is is the index strength, P is the load at failure and D is the distance between loading points at failure. The corrected index strength for 50 mm diameter samples (Isc) was obtained by using a correction chart (Broch and Franklin, 1972). On figure 2.22 and 2.23 the point load strength is plotted against %TOC and I_Q/I_I respectively. Although data is quite scattered point

SAMPLE NO	BOREHOLE	DEPTH (M)	DIRECTION OF LOADING	I_s (MPa)	$I_{sc}(50)$ (MPa)	%TOC	I_Q/I_I	FAILURE MODE
PL-1	KP-27	29.95	DIAMETRIC	2.2	2.0	5.0	-	EXTEN
PL-2	KP-28	21.94	"	0.1	-	6.7	-	" "
PL-3	KP-23	37.94	"	0.3	0.3	9.2	-	" "
PL-4	KP-27	22.24	"	0.1	-	8.6	-	" "
PL-5	KP-28	22.12	"	1.3	1.2	9.0	-	" "
PL-6	KP-23	37.98-38.03	AXIAL	6.9	-	-	-	CHIPPED
PL-7	KP-23	21.33-21.37	"	3.7	-	-	-	" "
PL-10	KP-23	26.48-26.50	"	17.9	16.7	10.2	7.8	EXTEN
PL-11	KP-15	56.30-56.32	"	14.7	13.7	12.7	7.6	" "
PL-12	KP-28	21.94-21.96	"	17.8	16.6	10.1	9.9	" "
PL-13	KP-22	25.37-25.39	"	17.7	16.5	6.1	11.3	" "
PL-14	KP-22	14.88-14.91	"	-	-	-	-	CHIPPED
PL-15	KP-17	76.13-76.15	"	9.8	9.1	5.8	8.3	EXTEN
PL-16	KP-23	21.54-21.56	"	13.1	12.2	5.6	9.2	" "
PL-17	KP-27	29.77-29.79	"	14.3	13.3	5.3	10.3	" "
PL-18	KP-27	29.80-29.82	"	16.2	15.1	6.0	9.3	" "
PL-19	KP-16	62.53-62.55	"	21.0	19.6	4.0	13.5	" "
PL-20	KP-16	25.12-25.14	"	10.8	10.1	8.8	5.2	" "

Table 2.4 Point load strength test data - test results.

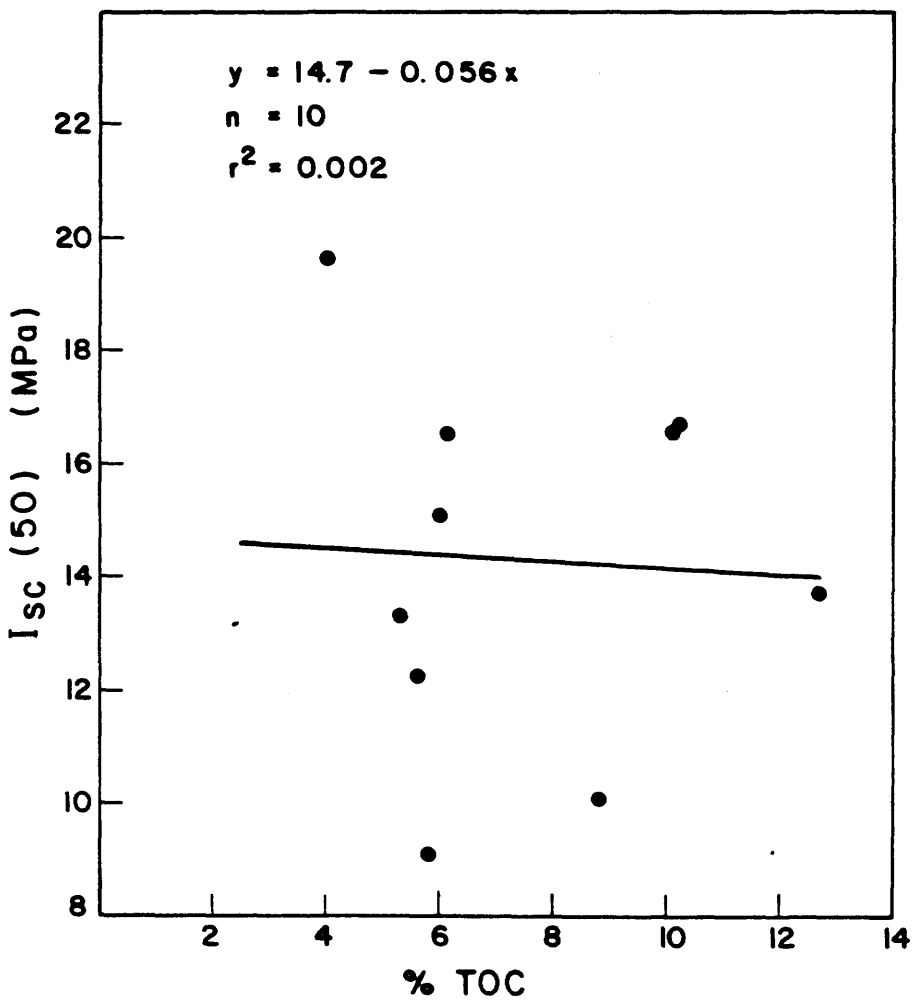

Figure 2.22 Corrected point load strength versus percent TOC.

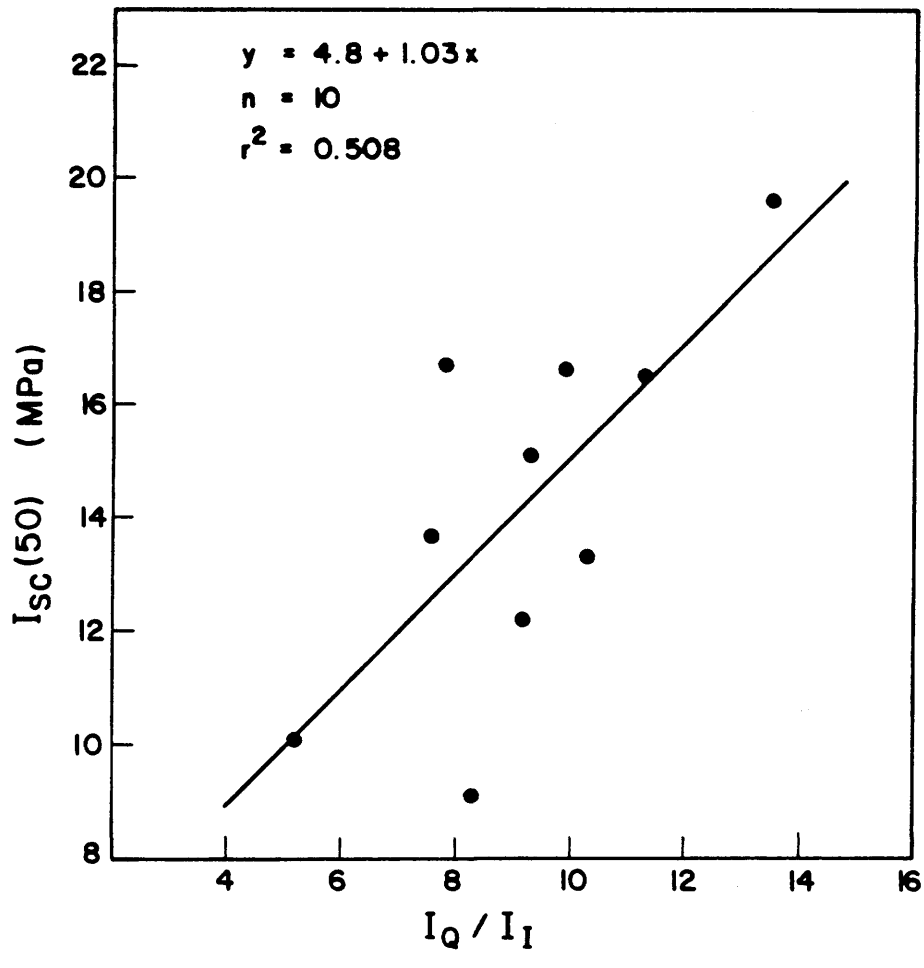

Figure 2.23 Corrected point load strength versus X-ray maximum intensity ratio of quartz and illite.

load strength is definitely influenced by the mineral matter and not (or to a much lesser degree) by the organic content. Linear regression yielded the following:

$$Isc = 14.7 - 0.06(TOC) \quad (MPa) \tag{28}$$

$n = 10$

$r^2 = 0.002 \quad (\alpha = 1.00)$

$$Isc = 4.8 + 1.03(I_Q/I_I) \quad (MPa) \tag{29}$$

$n = 10$

$r^2 = 0.508 \quad (\alpha = .055)$

By comparing the above regression equation for point load strength and X-ray intensity ratio of quartz and illite to those earlier obtained for uniaxial compression strength, the following relationship can be derived:

$$\sigma_u = 6.2(Isc) \tag{30}$$

The coefficient of 6.2 is a much lower value than normally observed (σu = 24(Isc)) in correlation of point load strength to the unconfined compressive strength. The high dependency of the point load strength index to the height to diameter ratio of the samples can explain this big difference (Broch, 1983). The above relationship is therefore only valid for samples tested for point load strength at height to diameter ratio of approximately 1/2. Due to the inherent weakness of the bedding planes the anisotropy index is very high but can not be assigned a value. This is usually the case for a material with inherent bedding plane fissility. The above relationship remains valid, however, because the major failure mode in uniaxial compression test was axial or subaxial splitting which is dominated by tensile effects.

2.6 Direct Shear Test Data

2.6.1 Sample preparation and test procedure

Originally it was intended to test unfractured samples at different normal loads but due to the high shearing resistance of this oil shale and the limitation of the loading apparatus (3000lb = 13.3 kN), samples could only be tested under normal stress of less than 0.6 MPa. After a few samples it was decided to terminate further testing of unfractured samples and rather concentrate on actual residual or ultimate frictional strength of existing fractures.

Samples were cut from the provided rock cores of appropriate length, 3.0 to 4.0 cm, for the shear box. Ends were ground flat and parallel, and dimensions measured and recorded along with a brief sample description. Unfractured samples were placed in the shear box and loaded at a constant displacement rate of 1.2 mm/min. The normal load was applied through a 1:10 lever arm and load against displacement was monitored on a chart recorder. Testing was carried on past the peak strength to obtain the ultimate frictional strength of the samples at a particular normal load. Fractured samples were prepared in the same manner, but for some samples a fracture was introduced by cutting the sample with a diamond saw and sanding the cut surface with sandpaper to introduce a controlled degree of roughness to the fracture surface. The samples were then placed in the shear box and tested at the same rate of loading as unfractured samples. Each sample was tested a few times at different normal loads. By doing this an ultimate failure envelope could be drawn for each of the tested samples.

2.6.2 Test results

Test results are tabulated in table 2.5 and 2.6 and plotted up as a function of the normal stress on figure 2.24. On figure 2.25 the peak strength of the unfractured samples is plotted against the X-ray intensity ratio of quartz and illite. As seen on the figure, data is scattered and regression analyses yielded the following equation which has an unacceptable confidence level:

$$t_p = -7.3 + 1.29(I_Q/I_I) \quad \text{(MPa)} \tag{31}$$

$\sigma n = 0.3$ MPa

$n = 8$

$r^2 = 0.454 \quad (\alpha = .18)$

No statistical relationship of any kind was found to exist between the %TOC and strength values. The ultimate frictional strength of a fracture did not seem to be very much influenced by the mineral matter but rather was a function of the surface roughness of the fracture. As noted from the results in table 2.6 and as seen on figure 2.24 a 600 grit fracture surface gives the lowest values for shear strength at a given normal stress but the natural rough fracture the highest. This is in accordance with theoretical and experimental results elsewhere. However, one can expect variations due to mineralogy for those fractures which have identical roughness coefficients. The following equations were derived through regression analyses of the data:

$$\tau_f = 0.44\sigma n^{0,97} \quad \text{(MPa)} \quad \text{(600 GRIT)} \tag{32}$$

$$\tau = 0.66\sigma_n^{0,95} \quad \text{(MPa)} \quad \text{(80 GRIT)} \tag{33}$$

$$\tau = 0.96\sigma_n^{0,90} \quad \text{(MPa)} \quad \text{(NATURAL ROUGH)} \tag{34}$$

As indicated by these equations dilatency is the governing shear strength parameter at the tested normal stresses and shearing of asperities is little involved. Shearing of asperities becomes more dominant by increasing normal stress, especially for the rough natural fracture, as indicated by the lower

SAMPLE NO	BOREHOLE	DEPTH (M)	τ_p (MPa)	τ_f (MPa)	σ_n (MPa)	%TOC	I_O/I_I
SH-1	KP-27	20.19-20.22	2.8	0.2	0.3	7.5	8.6
SH-2	KP-23	37.90-37.93	3.5	0.3	0.3	4.2	8.6
SH-3	KP-23	37.74-37.77	3.3	0.4	0.3	4.5	9.6
SH-4	KP-27	22.16-22.19	1.6	0.3	0.3	5.9	7.0
SH-5	KP-23	37.85-37.88	4.8	0.2	0.3	6.6	10.1
SH-6	KP-22	14.90-14.93	7.5	0.2	0.3	7.7	9.7
SH-7	KP-28	16.32-16-35	5.7	0.3	0.3	6.5	8.8
SH-8	KP-28	16.36-16.40	5.1	0.6	0.6	-	6.6
SH-9	KP-22	15.03-15.06	4.9	0.3	0.3	-	9.4
SH-10	KP-23	21.40-21.43	9.9	0.5	0.6	-	8.4

Table 2.5 Direct shear test data - test results of unfractured samples.

SAMPLE NO	BOREHOLE	DEPTH (M)	τ_f (MPa)	σ_n (MPa)	$\tau_f = a\sigma_n^b$ (MPa)	I_0/I_I	FRACTURE TYPE
SH-11a	KP-22	15.03-15.06	0.62	0.62	$\tau_f = 0.97\sigma_n^{0.90}$	9.4	NATURAL
"	"	"	1.18	1.23		"	"
"	"	"	1.70	1.85		"	"
"	"	"	2.19	2.47		"	"
"	"	"	2.66	3.09		"	"
"	"	"	3.11	3.70		"	"
SH-11b	KP-22	15.03-15.06	0.42	0.62	$\tau_f = 0.66\sigma_n^{0.92}$	"	80 GRIT
"	"	"	0.86	1.23		"	"
"	"	"	1.17	1.85		"	"
"	"	"	1.52	2.47		"	"
"	"	"	1.86	3.09		"	"
"	"	"	2.18	3.70		"	"
SH-12a	KP-23	21.50-21.53	0.42	0.62	$\tau_f = 0.67\sigma_n^{0.96}$	"	80 GRIT
"	"	"	0.82	1.23		"	"
"	"	"	1.21	1.85		"	"
"	"	"	1.59	2.47		"	"
"	"	"	1.96	3.09		"	"
"	"	"	2.32	3.70		"	"
SH-12b	KP-23	21.50-21.53	0.25	0.62	$\tau_f = 0.40\sigma_n^{0.97}$	"	600 GRIT
"	"	"	0.48	1.23		"	"
"	"	"	0.72	1.85		"	"
"	"	"	0.96	2.47		"	"
"	"	"	1.18	3.09		"	"
"	"	"	1.41	3.70		"	"
SH-13a	KP-27	29.82-29.85	0.41	0.62	$\tau_f = 0.65\sigma_n^{0.95}$	"	80 GRIT
"	"	"	0.79	1.23		"	"
"	"	"	1.16	1.85		"	"
"	"	"	1.52	2.47		"	"
"	"	"	1.88	3.09		"	"
"	"	"	2.23	3.70		"	"
SH-13b	KP-27	29.82-29.85	0.30	0.62	$\tau_f = 0.48\sigma_n^{0.96}$	"	600 GRIT
"	"	"	0.59	1.23		"	"
"	"	"	0.86	1.85		"	"
"	"	"	1.13	2.47		"	"
"	"	"	1.41	3.09		"	"
"	"	"	1.69	3.70		"	"

Table 2.6 Direct shear test data - test results of fractured samples.

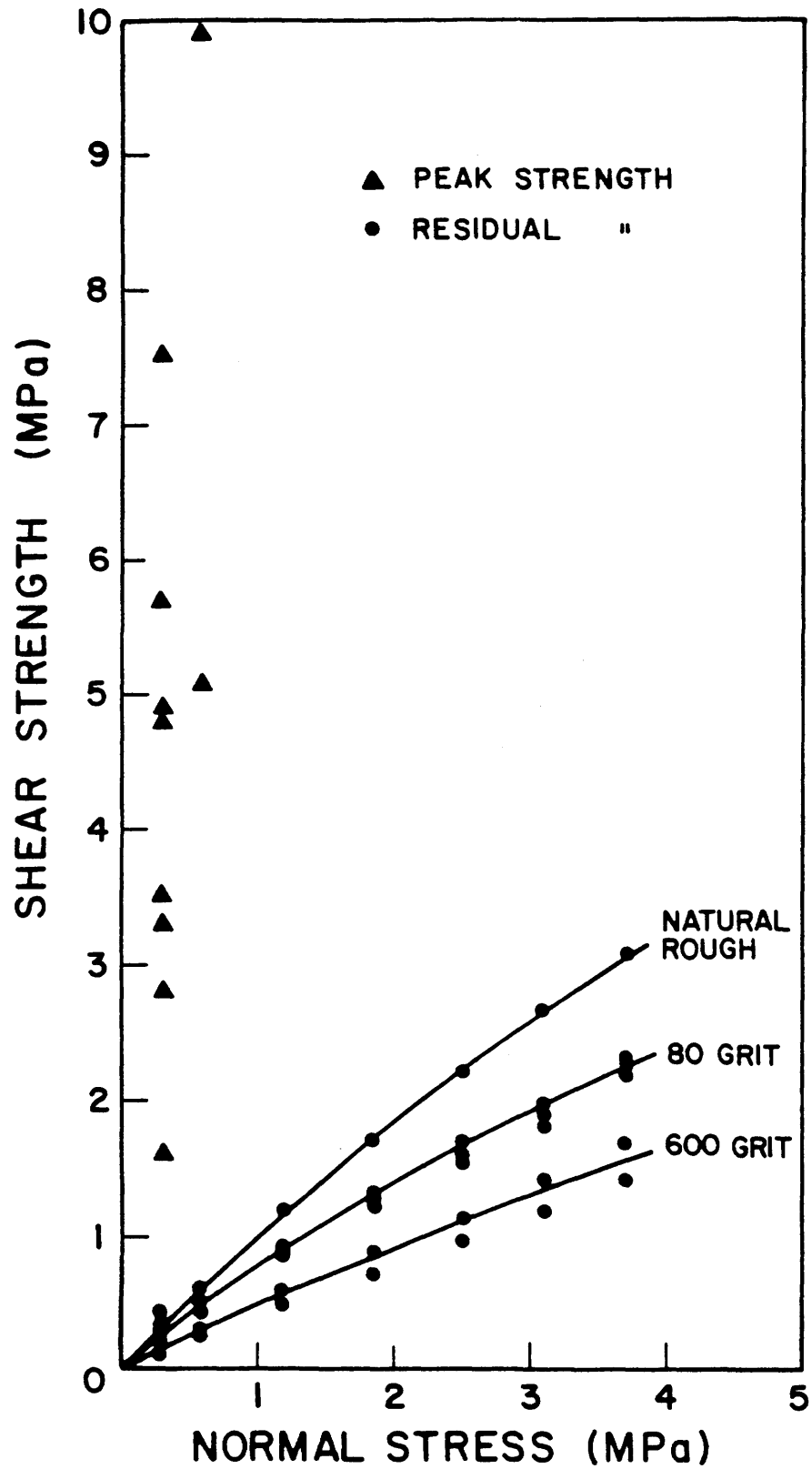

Figure 2.24 Direct shear strength versus normal stress.

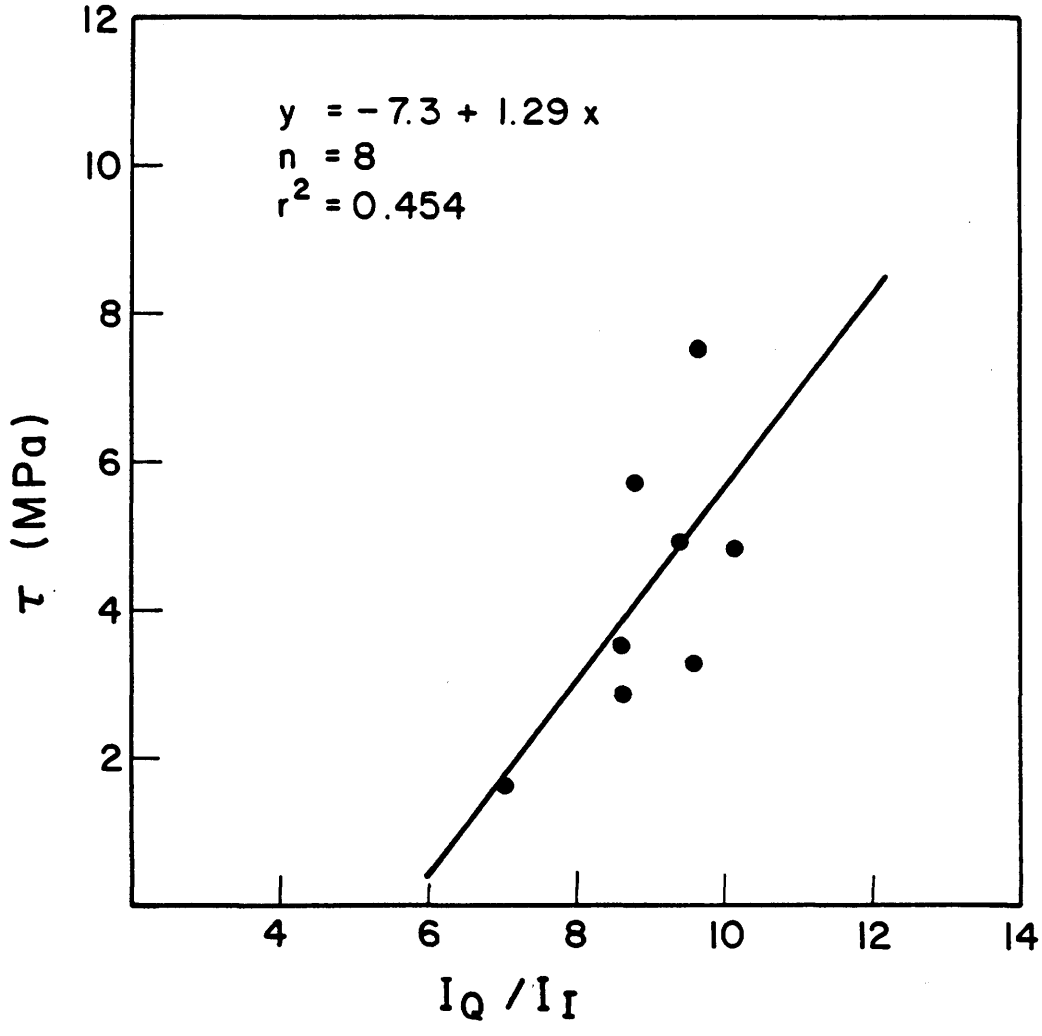

Figure 2.25 Direct shear strength of unfractured samples versus the X-ray maximum intensity ratio of quartz and illite.

power coefficient. Mineralogical variations are also partly involved.

No correlation data are given because of the strong autocorrelation of the two variables which would simply yield an extremely high value of r^2.

3.0 DISCUSSION

3.1 Factors Influencing Rock Strength

3.1.1 Extrinsic and intrinsic factors

Factors that influence the mechanical behavior of rock samples in laboratory testing and the obtained results can be divided into two groups: extrinsic factors and intrinsic factors. The extrinsic factors are those which are introduced from the environment during collection, preparation, and testing of the rock samples. These include effects due to variation in moisture, temperature, rate of loading, and geometry of the sample and effects introduced by the test apparatus and platens in contact with the rock sample. A comprehensive description of these factors can be found elsewhere (Vutukuri et al., 1974; Lama and Vutukuri, 1978).

The intrinsic factors are those which can be related to the internal structure and composition of the rock material and include: fabric, cracks, pores, and mineral composition. Rocks are inhomogeneous materials and these intrinsic factors have no less influential effects on rock behavior than factors introduced by the environment (Montoto, 1983; Mandzic, 1979). In the investigation described herein standard procedures were followed in sample preparation and test performance.

3.1.2 Influence of organic content

Besides anisotropy, there are two intrinsic parameters that are most commonly considered as being associated with variations in the mechanical properties of oil shales: organic matter content and mineralogy.

For the Green River Formation in the United States, the organic matter has been successfully correlated to the strength/deformation properties, whereas the influences of mineral matter is less obvious or relatively unimportant. The organic matter is always considered as having primary control on material properties. As the organic matter increases it dilutes and weakens the mineral-supported matrix and reduces the ability of the rock to resist higher stresses.

For the Green River Formation the organic matter is embedded in the carbonate/illite matrix and the range in organic matter content is great, ranging from 0 to 60 %Oc by volume. For the Kettle Point Formation the organic matter occurs only in the interstices and the range is much lower, 0 to 20 %Oc. Because of these fundamental differences the influence of organic matter on strength and deformation properties of the Kettle Point Formation are never felt in an atmospheric environment (normal temperature and chemistry).

3.1.3 Influence of mineralogy

In the oil shale literature the influences of mineral matter on material properties have been postulated (Chong et al., 1982). For example, the variation in material properties between the different members or zones of the Green River Formation has been explained in terms of differences in mineralogy. Also, more scatter of data points for low grade shales of the same formation, when plotted against the percent organic matter, is explained as being mainly due to mineralogical variations. These conclusions have never been rigorously tested in a large study, but are reasonably postulated.

The results presented in chapter 2 clearly indicate that mineral matter rather than organic matter has a dominant influence on the mechanical behavior of the Kettle Point Formation and, despite the qualitative nature of the X-ray technique used, maximum peak intensity ratio of quartz and illite is a useful indirect measurement of material properties and relates to physical behavior in a similar manner as %Oc is used for the Green River Formation in the United States.

By correlating the mechanical properties to the intensity ratio, interpretation of test results is much more consistent and material properties obtained in different tests can be more easily related to each other. For example, uniaxial compressive strength is approximately 9.3 times greater than the Brazilian tensile strength and approximately 6.2 times greater than the point load strength index, at the same quartz:illite intensity ratio. The latter number (6.2) is a much lower number than normally observed in comparison of point load strength to the uniaxial compressive strength. Sensitivity of point load strength index to height/diameter ratio explains this difference (Broch, 1983).

A question may arise as to whether the X-ray intensity ratio is an acceptable quantitative indirect measurement of actual mineral variation and if a more precise mineralogical analysis is required. This is a valid argument, but various factors indicate that the X-ray intensity ratio, as used, is an acceptable substitute for other much more complicated and time consuming techniques. Quartz and illite usually compose more than 85% of the mineral matter. Quartz and illite are most commonly analyzed quantitatively by X-ray diffractometry using internal standards. There is no reason to believe that a single mineral analysis can be substituted for the intensity ratio to obtain better correlation coefficients. Both minerals (quartz for increase and clay for decrease) are involved in reducing (increasing) the cohesion (grain interlocking) and internal friction (particle-to-particle friction) of the material. In fact the coefficients of determination in regression analyses alone are a strong indicator of the reliability of the X-ray intensity ratio as a satisfactory correlate to material properties of the Kettle Point Formation.

The main drawback to the expressed intensity ratios is the reproducability of obtained values. Our tests do indicate that strong functional relationships exist between the ceramic tile method and the conventional powder press method and that practically none of the diffraction patterns originated from the ceramic tile.

The relationship between the quartz:illite ratio and strength or deformation properties can be explained in the following manner. Quartz and illite (or hydrous mica) provide the structural matrix of the material but the organic matter occurs dominantly or only in the interstices. The organic matter therefore has little effect on strength and deformation properties under atmospheric conditions. Increasing amounts of clay or mica platelets,

however, reduce the particle to particle friction and degree of interlocking of the quartz grains and thus reduce the ability of the rock matrix to resist high stresses. Also illite has a lower residual friction angle than quartz, so ultimate rock strength will also be affected in a similar manner.

3.1.4 Thermal influences and the organic material

For the Green River Formation it is noted that thermal conductivity decreases with increasing organic content (Rajeshwar et al., 1979). A similar hypothesis is likely to hold for the Kettle Point Formation because the organic matter is a poorer conductor of heat than the inorganic constituents of the oil shale matrix. Thermal expansion and thermal spalling increases with increasing organic content due to the generation of CO_2 gas pressure upon combustion of the organic matter. The gas pressure creates structural weaknesses in the rock matrix. The weakness is induced by local elevated pore pressure which cannot be released rapidly enough to avoid local minor attack of the rock fabric by the rupture of the weaker grain-to-grain bonds. The low absolute permeability of the matrix, combined with the impedance effect of the organic matter on relative gas permeability, inhibits gas pressure dissipation. The organic matter has therefore a very active influence on thermal properties and the change in material properties upon heating.

3.2 On Reliability of Test Results

3.2.1 Size of sample body

Usually, the larger the sample body, the better and more reliable is the interpretation of results. This is, however, not always the case and a financially better alternative often is to test fewer samples covering a wider

range of formation characteristics than many samples of the same or similar characteristics. For example, the mechanical properties of the Kettle Point Formation, as described herein and in prior research, are derived mainly from testing of solid intact core samples but the heavily jointed intervals are left out because specifications of sample size and shape are not met.

Correlation of material properties to some intrinsic parameter which can be reliably related to the physical characteristics can be used to give an estimate of the physical or mechanical properties of those untested intervals. Also, any correlation that exists between intrinsic properties and material properties can be used to compare results of different types of tests on the same material and can possibly be used to extend results from individual tests beyond the tested interval. For the Kettle Point Formation the X-ray intensity ratio of quartz and illite provides such a relationship. It can be used to get more comprehensive evaluation or estimates of the variation of material properties within the formation and therefore reduces the requirements for a very large sample body. Also, because of the functional relationship that exists between the individual tests and the consistency in test results, the small sample body used herein is considered adequate.

3.2.2 Errors in measurements

The measurement error is relatively small and can be easily estimated. For example, in the Brazilian test, allowable error in dimension measurements was $\pm$ 0.1 mm for the diameter and $\pm$ 0.2 mm for the thickness of the disc. The error involved in measuring the peak load from the graphical display of load against displacement was about 100 N. The combined effect that these errors would have on the calculated tensile strength (σ_t) would be of the order $\pm$ 0.1 to 0.2 MPa, which is well within 5% of the reported

value. This range is reasonable for tensile data.

Similarly, it can be shown that errors involved in calculating compressive strength (σ_1) in uniaxial and triaxial compression test are between $\pm$ 1 to 2 MPa and for Young's modulus between $\pm$ 0.2 to 0.4 GPa, again less than 5% of the reported value. For the direct shear test the error is also within 5% but for the point load test the error is slightly greater, 5% to 10%. Errors of this order are reasonable in tests like these and are not likely to have a significant effect on the use of the test results.

3.2.3 Errors due to test methodology

Unfortunately, measurement errors are not the only errors involved. If data obtained in this investigation are compared to data obtained by Kim (1978), mentioned in chapter 1.3, it seems that Kim's values are slightly greater. The difference, however, is considerably reduced if one considers only true, low modulus, oil shale samples and no 'cap' or 'floor rocks'. Also one has to consider that the rate of loading is quite different. Wheras Kim (1978) used a loading rate of 0.69 MPa/sec the loading rate in this investigation is displacement controlled, being approximately 5×10^{-6} sec^{-1}. For linear elastic material, stress rate and strain rate are related through the following equation:

$$d\sigma/dt = d\varepsilon/dt \times E \qquad (35)$$

By substituting proper values into above equation it can be deduced that Kim's rate of loading was approximately an order of magnitude greater than that used for this investigation and, as mentioned earlier, the general tendency is for increasing strength with increasing rate of loading. Other factors could also be involved such as those due to differences in geometry and moisture conditions (for example, Kim used air-dried samples).

Although comparison is quite difficult, because of the poor reliability in using %TOC or %wt loss as a measure of strength and deformation properties, it can be roughly estimated that the results for uniaxial compression tests presented in the previous chapter are no more than 15% lower than the values obtained by Kim (1978) and the difference can partly be explained as due to the difference in rate of loading and moisture conditions within the samples.

Comparison of the point load strength data to those obtained by Kim (1978) indicates that the relative difference is small. The values reported in previous chapters are all within the range reported by Kim (1978), but again because of poor reliability of %TOC as a indirect measure of strength, an exact comparison is difficult to accomplish.

3.2.4 Regional variation in lithology

The samples tested from the Kettle Point Formation are all from areas in south-western Ontario and therefore at the edge of the Michigan Basin. The samples tested by Kim (1978) and Singh (1979) were from areas closer to the center of the Basin. Regional variation in lithology can therefore exist, although mineralogical similarities are evident, and may be involved in the differences in strength and deformation properties. Also, depth of burial is quite different. Most of the samples used in this investigation were from depths of less than 50 metres whereas the samples tested by Kim (1978) were from a depth interval of 400 - 460 m. Increasing crystallinity of clay minerals (illite) and reduced porosity due to burial and diagenesis might be reflected by increases in mechanical strength and moduli.

3.3 Comparison to other Materials

3.3.1 Devonian oil shales in eastern United States

The comparison of the Antrim Formation to the Kettle Point Formation has already been summarized. Similarities exist not only in mineralogical and geological characteristics but also in physical and mechanical properties. Regional variations in lithology and test methodology can account for the small differences that are observed.

Other equivalent Devonian oil shales in the eastern United States also show similar mechanical behavior. Tests conducted on the New Albany Shale in southern Indiana yielded values of Brazilian tensile strength from 1.1 - 17.6 MPa with an average of about 9 MPa which is quite similar to results obtained in this investigation. Sonic velocity tests of the same formation yielded values of P- and S-wave velocity at an average ratio of about 1.7 which is similar to results from the Antrim Formation (Blakely et al., 1981).

3.3.2 Green River Formation

Despite the difference in origin and mineral composition, certain similarities exist between the Kettle Point Formation and the Green River Formation. Both deposits are classified as being of low modulus ratio and the ratio of tensile strength to uniaxial strength is similar, around 1/10. In triaxial compression, the angle of internal friction covers a wide range, 10^0 to 50^0 for the Green River Formation and 20^0 to 40^0 for the Kettle Point Formation, and in both cases variations are due to the intrinsic material properties.

In other aspects these two deposits are quite different. For example, for samples of similar organic contents, uniaxial compressive strength and modu-

lus of deformation of the Green River Formation are slightly higher (20% - 30%) than for the Kettle Point Formation. The Green River Formation is usually well stratified and does not generally exhibit fissility, whereas the Kettle Point oil shale is highly fissile and has a very low tensile strength across its bedding planes. A more important fact is the mineralogical difference. Carbonate minerals, calcite and dolomite, decompose endothermally under retorting conditions, whereas quartz is unaffected. On the other hand high quartz contents might indicate more abrasion and wear problems during drilling and on tunnelling equipment.

3.3.3 Other rock materials

The Kettle Point Formation can be categorized along with other low porosity sedimentary and low metamorphic rocks having uniaxial compressive strengths commonly between 50-100 MPa and, if still brittle, differential stress of 200-300 MPa at 100 MPa confining pressure (Paterson, 1978). This categorization can be narrowed somewhat, as discussed in chapter 3.4, by considering other material properties such as modulus of elasticity.

In comparison to other shales in southern Ontario the Kettle Point Formation has a compressive strength (perpendicular to bedding) and tensile strength (parallel to bedding) in the upper range of reported values (Lo et al., 1976; Russell and Gale, 1982; Franklin and Gruspier, 1983). The Kettle Point Formation has, however, a lower modulus ratio than most of the Ontario shales, due to the high fissility of the shale along the bedding planes. Two slake durability tests were performed on the Kettle Point Formation. The durability index, after two cycles of wetting and drying, was more than 98% which is higher than for most other shales in Ontario (Russell, 1982; Russell and Gale, 1982; Franklin and Gruspier, 1983).

3.4 Material Classification

3.4.1 Geological classification

The Kettle Point Formation would be classified as being a clastic, fine-grained sedimentary rock, containing organic material. The rock is laminated and has the appearance and structural characteristics of most common shales but lacks the required amount of clay minerals to be called a true shale. The large amount of silt-sized quartz grains indicates that the material should be classified as quartzitic silty-shale containing organic matter (kerogen) rather than oil shale. The term oil shale has, however, become established in the literature and it is not detrimental in engineering applications use.

3.4.2 Engineering classification

The conventional geological classification of rock types is often insufficient for engineering purposes. Besides the geological and petrographical descriptions of the rock, a qualitative estimate of strength, hardness, anisotropy, and durability is often required. Laboratory testing on intact rock samples can provide information on some of these parameters. The classification system suggested by Deere and Miller (1966) that compares modulus of elasticity to uniaxial compressive strength is an example of a more general engineering classification system for rock types. As shown on figure 3.1 the Kettle Point oil shale falls in the category of low modulus, medium strength rocks. On the same figure, for comparison, a shaded area denotes the category in which shales most commonly occur (Deere and Miller, 1966). Another classification system for oil shales, suggested by Bieniawski (1973), compares oil yield to uniaxial compressive strength, and the Kettle Point oil

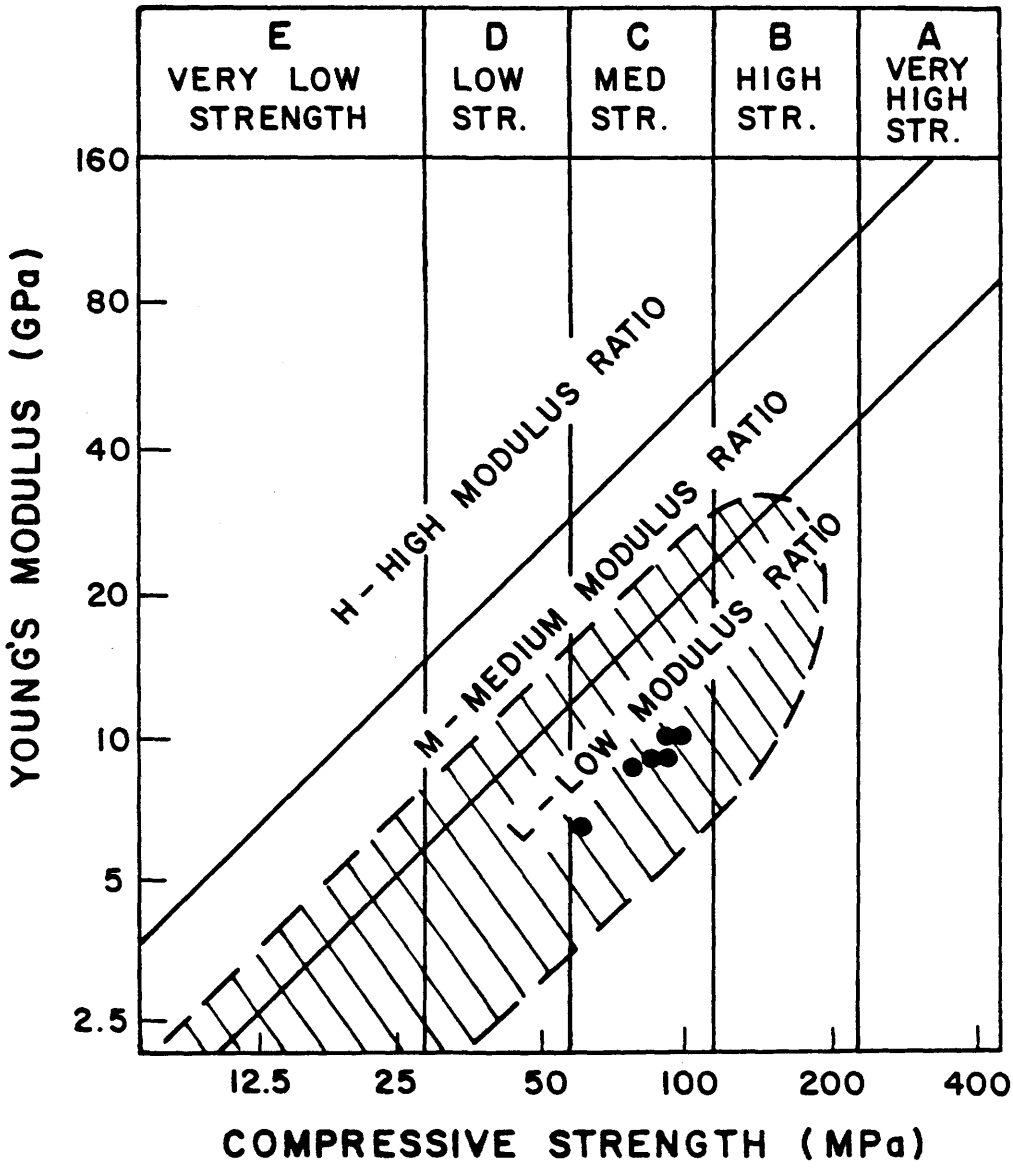

Figure 3.1 Classification of the Kettle Point Formation according to Deere and Miller (1966).

shale would be classified as being a moderately strong (50 to 100 MPa) rock of oil yield less than 100 l/tonne. For comparison, the Green River Formation would be classified as being of rather high strength (100 - 200 MPa) for the same oil yield. A third oil shale deposit, Puertollano, Spain, would be classified as being of low strength (25 - 50 MPa) at the same oil yield

(Berzal et al., 1983). All these oil shale deposits are, however, classified as being of low modulus ratio.

Many other classification systems exist but often they are based on field observations and core logging, and parameters such as jointing, fracture spacing, etc., are included in the classification scheme. These were not obtained for this report. For the Kettle Point Formation a few important facts are worth noting such as the high quartz content which might indicate wearing and abrasion problems during tunnelling operations. Also, a potential high degree of anisotropy of mechanical properties might change as a function of the direction of loading with respect to bedding planes.

TYPE OF TEST	RANGE IN VALUES	DERIVED RELATIONSHIPS
Brazilian Tensile	σ_t=5.1-16.5 MPa $\bar{x}$ = 9.3 s=2.2	σ_t=2.2+0.82 (I_Q/I_I) r^2=0.750
Uniaxial Comp.	σ_u=59-100 MPa $\bar{x}$ = 83 s = 14 E_t=5.9-10.1 GPa $\bar{x}$ = 8.5 s =1.4 ν = 0.19-0.29 $\bar{x}$ = 0.24 s=0.03	σ_u=23.0+7.20(I_Q/I_I) r^2=0.609 E_t=2.7+0.73 (I_Q/I_I) r^2= 0.693
Triaxial Comp.	σ_{1p}=85-164 MPa σ_3=1.7-20.7 MPa σ_{1p}=26-91 MPa ϕ_p = 20° - 36° ϕ_f = 20° - 34° C = 22-26 MPa	τ_{mp}=21.0+0.059(σ_{mp})(I_Q/I_I) r^2= 0.949 τ_{mf}=6.6+0.056(σ_{mf})(I_Q/I_I) r^2= 0.972
Point Load St.	I_{sc}=9.1-19.6 MPa $\bar{x}$ = 14.3 s=3.3	I_{sc}=4.8+1.03(I_Q/I_I) r^2= 0.508
Direct Shear	τ_p=1.6-7.5 MPa $\bar{x}$ = 4.3 s=1.9 σ_n = 0.3 MPa τ_f=0.2-3.1 MPa σ_n =0.6-3.7 MPa	τ_p=7.3+1.29(I_Q/I_I) r^2=0.454 σ_n=0.3 MPa τ_f=0.44 $\sigma_n^{0.97}$(v. smooth) τ_f=0.96 $\sigma_n^{0.90}$(v. rough)

$\tau_{mp}=(\sigma_{1p}-\sigma_3)/2$ $\sigma_{mp}=(\sigma_{1p}+\sigma_3)/2$ $\tau_{mf}=(\sigma_{1f}-\sigma_3)/2$ $\sigma_{mp}=(\sigma_{1f}+\sigma_3)/2$

subscript p denotes peak values of unfractured samples

subscript f denotes residual or ultimate frictional values of a fracture

Table 4.1 Test results summarized

4.0 SUMMARY AND CONCLUSIONS

4.1 Summary of Test Results

In contrast to other studies of the Devonian black shales of the eastern United States (Antrim Formation) our data do not indicate that the material properties are to any extent influenced by the organic matter within the sample domain. However, a very strong dependency was found to exist between strength and deformation properties and the mineral ratio of the two main mineral constituents composing the rock, quartz and illite (Table 4.1). The mineral ratio is expressed as X-ray maximum intensity ratio of these two minerals and we believe that there exists a functional relationship between the actual mineral ratio and the X-ray intensity ratio. The fact that influences of organic matter are not observed for the Kettle Point Formation as for the Green River Formation in the United States can be explained as being mainly due to the small amounts, and small range, of organic material within the Kettle Point Formation (10 - 20 %Oc), whereas the range is much greater for the Green River Formation (10 - 60 %Oc). Also, the Kettle Point Formation is strongly supported by a structural matrix where quartz along with illite compose the matrix structure and organic matter is only in the interstices or as inactive grains, whereas for the Green River Formation, carbonate minerals along with clay minerals provide a structural support to the matrix only for the material containing the lowest amounts of organic matter.

Observed Brazilan tensile strength ranged from 5.1 to 16.5 MPa and increased in a linear fashion with increasing X-ray intensity ratio of quartz and illite. Uniaxial compression strength can be expressed as being approxi-

mately 9.5 times the Brazilian strength and increased similarly, as a linear function of the X-ray intensity ratio. The ratio of modulus of deformation, or Young's modulus, to the uniaxial compressive strength is about 100, classifying the rock as being of low modulus ratio. Modulus of deformation also increases linearly as a function of the X-ray intensity ratio of quartz and illite. Poisson's ratio along with offset strain were the only parameters that did not indicate a functional relationship to the mineral ratio of quartz and illite. In triaxial compression the compressive strength increased normally with increasing confining pressure. The amount of increase is also functionally related to the mineral ratio of quartz and illite.

Angles of internal friction and cohesion ranged from 20 to 36^0 and 22 to 26 MPa for the X-ray intensity ratio of 6 to 10 respectively. The modulus of deformation was little influenced by increasing confining pressure which is typical of strong stiff material of low porosity. The offset strain, which can be used as an indirect measurement of ductility, increased by a factor of approximately $0.01\sigma_3^{2,1}$ with increasing confining pressure. Point load strength was about 1/6 of the uniaxial compression strength and was also functionally related to the mineral or X-ray intensity ratio of quartz and illite. Direct shear strength of unfractured samples yielded shear strengths ranging from 1.5 to 9.9 MPa for normal stress of 0.3 and 0.6 MPa. Further testing at higher stresses had to be terminated because of the apparatus limitations. Direct shearing of natural and created fractures indicated that roughness of the fracture surface, rather than variations in the mineral or organic matter, had the greatest effect on the ultimate strength of the fracture. Influences of mineral matter are, however, expected for fractures of identical surface roughness.

A very important characteristic of the Kettle Point Formation is the extreme inherent weakness of the bedding planes. It is a property that causes great difficulties in sample preparation and might cause problems in stability of mine openings but could ease the creation of horizontal fractures in hydraulic or explosive operations. The least principal compressive stress in situ (σ_3) is almost certainly vertical, and therefore, in the upper hundred metres, the stress regime will predicate horizontal fractures.

4.2 Mineability

4.2.1 Undergound mining

The Kettle Point Formation is a strong material, relatively speaking, and can be readily mined by underground methods. Because of its uniformity, tunnel boring machines can be easily designed to work at maximum efficiency for boring of adits and tunnels to develop a mine. The material is also sufficiently brittle to allow blasting, but the bedding plane fissility will cause problems, as blasting will damage some surrounding rock and significantly reduce what little tensile strength exists. This will lead to roof spalling and increase the density of rock bolts required for roof support.

The actual mining operation must be designed to minimize surrounding rock damage for several reasons. First it must be designed to minimize the aforementioned roof control problem. Second, if the underground space is to be used, the rooms must be stable for many years, even centuries, therefore there is an incentive to use some continous mining technique. However, techniques designed for coal and potash are insufficient, as equipment design is inadequate to cope with the fairly strong and likely abrasive Kettle Point Formation. Third, surface subsidence is to be minimized, and full room

integrity is required.

At relatively shallow depths, the width of room which can be maintained is quite wide. For a 3 to 7 metre opening, a height to width ratio of 5:1 to 3:1 is probably feasible, with intact pillars having a width to height ratio of 2.0. Further analyses are required, but it seems that, at depths less than 100 m, extraction ratios of at least 55% - 60% are reasonable. Roof support will be required using 1.5 to 2.0 metre rock bolts to pin the roof and avoid delaminations. The shale will not deteriorate in the presence of water nor will it desiccate and spall, therefore no direct protection of the shale is required (e.g. shotcrete or lining).

Uncertainities as to the frequency and character of vertical joints renders these observations a bit tenuous at present. Besides joints, post-depositional tectonics in the area have been identified (personal communication,D. Russell 1984, Ontario Geological Survey), but further studies of joints and tectonic features are required if mining operations are to be designed.

4.2.2 Surface mining

In the case of surface mining operations no problems whatsoever are expected from the Kettle Point Formation. In fact it is likely to be extremely stable, blastable, crushable, and trafficable in a quarrying operation. Whether surface mining is a likely operation in the heavily populated area of southwestern Ontario is, however, a matter that cannot be discussed herein.

5.0 FURTHER STUDIES

If the Kettle Point oil shale is to be further evaluated as a resource, multiple uses must be studied. The following list includes a number of relatively economical small studies which should be considered.

1. Abrasiveness and crushing behavior should be evaluated to assess feasibility of using underground continuous mining machines and to find out what mine product size is to be expected.

2. More detailed mineralogy is required to firm up the relationship between properties and quartz/illite contents.

3. A scanning electron microscope study using EDX and secondary electron emission mapping should help in identifying the habit of the organic matter and studying the grain-to-grain fabric of the quartz/illite matrix. This will serve to verify some of the hypotheses herein.

4. The behavior of the crushed material on heating should be tested, both to evaluate liquid product and to evaluate the potential use of the spent shale as light-weight aggregate.

5. The spent shale should be heated to 1100^{o}C to evaluate whether it will aquire pozzolanic properties. In continous forward flow retorting this cannot be readily achieved, but post-heating is easily accomplished. Addition of small quantities (<10%) of crushed limestone to the retorting material will aid in developing pozzolanic properties.

6. It is probably worthwhile to study the heavy metals and trace elements

found in the shales, as this has important geochemical ramifications for origin studies and for potential use analysis.

ACKNOWLEDGMENT

We wish to thank James Baleshta for suggestions and design of various testing equipment, George Farrell for assistance in carrying out experiments, Ralph Dickhout and Peter Churcher for carrying out TOC analyses, and Chris Fordham for editing of this report. Also we would like to thank Dave Russell for editorial comments and his coworkers at OGS for support and assistance during this project.

REFERENCES

Attewell, P.B., Taylor, R. K., 1973. Clay Shales and Discontinous Rock Mass Studies. Final Report to European Research Office, US Army on Contract no DA-ERO-591-72-G0005.

Barker, J. F., Dickhout, R. D., Russell, D. J., Johnson, M. D., Gunther, P., 1983. Paleozoic Black Shales of Ontario - Possible Oil Shales. ACS Symposium Series, No 230, Geochemistry and Chemistry of oil shales, pp. 119-138.

Bieniawski, Z. T., Hawkes, I., 1978. Suggested Methods for Determining Tensile Strength of Rock Materials. ISRM Commission on Standardization of Laboratory and Field Tests, Int. J. of R. M. and Min. Sci., Vol 15, No 3, pp. 99-103.

Bieniawski, Z. T., et al., 1979. Suggested Methods for Determining the Uniaxial Compressive Strength and Deformability of Rock Materials. ISRM Commission on Standardization of Laboratory and Field Tests, Int. J. of R. M. and Min. Sci., Vol 16, No 2. pp. 135-140.

Berzal, J. L., Oteo, C. S., Rodriquez-Ortiz, J. M., 1983. Geotechnical Properties of the Puertollano Oil Shale. ISRM 5th Int. Con. on Rock Mech. Proc., Melbourn, Austr., pp. A87-A91.

Blakely, R. F., Hasenmueller, N. R. (ed.), Woodard, G. S. (ed.), 1981. Studies of the New Albany Shale (Devonian and Mississippian) and Equivalent Strata in Indiana - Physical Tests. United States Departm. of Energy, Contract No. DE-AC 21-76MC05204, Morgantown Energy Technology Center, Morgantown, West Virginia, pp. 70-84

Broch, E., Franklin, J. A., 1972. The Point-Load Strength Test. Int. J. Rock Mech. Min. Sci., Vol 9, pp. 669-697.

Broch, E., 1983. Estimation of Strength Anisotropy using the Point Load Test. Int. J. Rock Mech. Min. Sci., Vol 20, No 4, pp. 181-187.

Chang, N. Y., Jumper, A. L., 1978. Multiple Stage Triaxial Test on Oil Shale. Proc. 19th U.S. Symposium on Rock Mech., Stateline, Nevada, May 1-3, pp. 520-522

Chong, K. P., Smith, J. W., Chang, B., Hoyt, P. M., Carpenter, H. C., 1976. Characterization of Oil Shale under Uniaxial Compression. 17th U.S. Symposium on Rock Mech., Proc. (USA), pp. 5C5.1-5C5.8

Chong, K. P., Ward, J., Chang, B., 1979a. Oil Shale Properties by Split Cylinder Method. J. Geotech. Eng. Div. ASCE, Vol 105, pp. 595-611.

Chong, K. P., Uenishi, K., Munari, A. C., 1979b. Three-Dimentional Characterization of the Mechanical Properties of the Colorado Oil Shale.

Proc. 20th U.S. Symposium on Rock Mech., Austin, Texas, June 4-6, pp. 369-379.

Chong, K. P., Hoyt, P. M., Smith, J. W., 1980. Effects of Strain Rate on Oil Shale Fracturing. Int. J. of Rock Mech. and Min. Sci., Vol 17, No 1, pp. 35-43.

Chong, K. P., Smith, J. W., Borgman, E. S., 1982. Tensile Strengths of Colorado and Utah Oil Shales. Journal of Energy (USA), Vol 6, No 2, pp. 81-85.

Closmann, P. J., Bradley, W. B., 1979. Effects of Temperature of Tensile and Compressive Strengths and Young's Modulus of Oil Shale. Society Petrolum Engineer Journal, Vol 19, No 5, pp. 301-312.

Costin, L. S., 1981. Material Properties of Green River Oil Shale. Sandia Report, Sand 81-1457.

Crookston, R. B., 1978. Mining Oil Shale. Underground Space, Vol 2, pp. 229-241.

Deere, D. H., Miller, R. P., 1966. Engineering Classification and Index Properties for Intact Rock. Air Force Weapons Laboratory Technical Report No. A FWL-TR-65-116. Kirtland, New Mexico.

Dusseault, M. B., Bradshaw, K. L., Ehret, K., Loftsson, M., 1983. Mechanical Properties of Oil Shales. OGS Open File Report, OFR 5472.

Fordham, C. J., Dusseault, M. B., 1983. Thermogravimetric Evaluation of Organic Contents of Oil Shales. Unpublished Paper.

Franklin, J. A., 1971. Triaxial Strength of Rock Materials. Rock Mechanics 3, pp. 86-98.

Franklin, J. A., Gruspier, J. E., 1983. Evaluation of Shales for Construction Projects - An Ontario Shale Rating System. Ontario Ministry of Transportation and Communication, Research Report RR229, pp. 12-25.

Hondros, G., 1959. The Evaluation of Poisson's Ratio and the Modulus of Materials of a Low Tensile Resistance by the Brazilian (Indirect Tensile) Test with Particular Reference to Concrete. Aust. J. App. Sci., Vol 10, pp. 243-268.

Humphrey, J. P., 1978. Extraction of Hydrocarbons from Antrim Oil Shale. 11th Oil Shale Symposium, Golden, Colorado, April 12-14, pp. 147-157.

Kim, K., 1978. Mechanical Characteristics of Antrim Shale. DOE Open File Report, FE-2346-24.

Lama, R. D., Vutukuri, V. S., 1978. Handbook on Mechanical Properties of Rocks - Testing Techniques and Results. Publ. Trans Tech Publications, Vol 2.

Lo, K. Y., Wai, R. S. C., Palmer, J. H. L., Quigley, R. M., 1978.

Time-Dependent Deformation of Shaley Rocks in Southern Ontario. Can. Geotech. Jour., Vol 15, pp. 537-547.

Mandzic, E., 1979. Generalization of Factors Effecting the Uniaxial Strength of Rock Material. ISRM 4th Int. Con. on Rock Mech. Proc., Swiss, Sept. 2-8, pp. 397-408.

Matthews, D. R., 1983. The Devonian-Mississippian Oil Shale Resource of the Eastern United States. 16th Oil Shale Symposium, Golden, Colorado, April 13-15, pp. 1-12.

McNamara, P. H., Peil, C. A., Washington, L. J., 1979. Characterization, Fracturing and True In Situ Retorting in the Antrim Oil Shale of Michigan. 12th Oil Shale Symposium, pp. 353-365.

Montoto, M., 1983. Petrophysics: The Petrographic Interpretation of the Physical Properties of Rocks. ISRM 5th Int. Con. on Rock Mech. Proc., Melbourn, Aust., pp. B93-B98.

Paterson, M. S., 1978. Experimental Rock Deformation - The Brittle Field. Publ. Spring-Verlag, Berlin, pp. 21-28.

Rajeshwar, K., Dubow, J. B., 1979. Thermophysical Properties of Devonian Shales. Soc. Pet. Eng. AIME, Annu. Fall Tech. Conf. Exhib., Pap. (USA), No 54, pp. 1-8.

Russell, D. J., 1982. Controls on Shale Durability: the Response of two Ordovician Shales in the Slake Durability Test., Can. Geotech. Jour., Vol 19, pp. 1-13.

Russell, D. J., Gale, J. E., 1982. Radioactive Waste Disposal in Sedimentary Rocks of Southern Ontario., Geoscience Canada, Vol 8, No 4, pp. 200-207.

Russell, D. J., Barker, J. F., 1984. Stratigraphy and Geochemistry of the Kettle Point Shale, Ontario., Proceedings of the Third Eastern Oil Shale Symposium, University of Kentucky, IMMR, in press.

Singh, S. P., Hockings, W. A., Kim, K., 1979. Change in Mechanical Properties of Antrim Oil Shale on Retorting. Proc. of the 20th U.S. Symposium on Rock Mech., Austin, Texas, June 4-6, pp. 363-368.

Skempton, A. M., 1964. Long Term Stability of Clay Slopes., Geotechnique, Vol 14, pp. 84-87.

Smith, J. W., 1976 Relationship between Rock Density and Volume Organic Matter in Oil Shales. ERDA Report of Investigation, LERC/RI-76/6.

Thorne, H. M., et al., 1964. Oil Shale Technology: A Review. U. S. Bur. of Mines, Rept. No 8216, p. 7.

Vogler, U. W., Kovari, K., 1978. Suggested Methods for Determining the Strength of Rock Material in Triaxial Compression. ISRM Commission on Standardization of Laboratory and Field Tests, Int. J. of Rock

Mech. and Min. Sci., Vol 15, No 2, pp. 47-51.

Vutukuri, V. S., Lama, R. D., Saluja, S. S., 1974 Handbook on Mechanical Properties of Rocks., Publ. Trans Tech Publications, Vol 1.